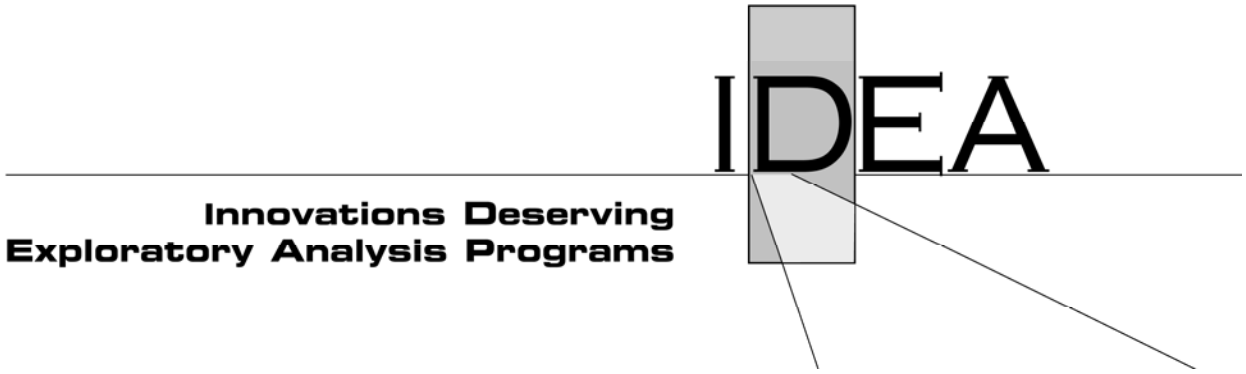

Highway IDEA Program

Asphalt Cement Testing with the Duomorph Asphalt Rheology Tester (DART)

Final Report for Highway IDEA Project 41

Prepared by:
J. Mallela and S.H. Carpenter, University of Illinois, Urbana-Champaign, IL

November 2000

TRANSPORTATION RESEARCH BOARD
OF THE NATIONAL ACADEMIES

INNOVATIONS DESERVING EXPLORATORY ANALYSIS (IDEA) PROGRAMS
MANAGED BY THE TRANSPORTATION RESEARCH BOARD (TRB)

This NCHRP-IDEA investigation was completed as part of the National Cooperative Highway Research Program (NCHRP). The NCHRP-IDEA program is one of the four IDEA programs managed by the Transportation Research Board (TRB) to foster innovations in highway and intermodal surface transportation systems. The other three IDEA program areas are Transit-IDEA, which focuses on products and results for transit practice, in support of the Transit Cooperative Research Program (TCRP), Safety-IDEA, which focuses on motor carrier safety practice, in support of the Federal Motor Carrier Safety Administration and Federal Railroad Administration, and High Speed Rail-IDEA (HSR), which focuses on products and results for high speed rail practice, in support of the Federal Railroad Administration. The four IDEA program areas are integrated to promote the development and testing of nontraditional and innovative concepts, methods, and technologies for surface transportation systems.

For information on the IDEA Program contact IDEA Program, Transportation Research Board, 500 5th Street, N.W., Washington, D.C. 20001 (phone: 202/334-1461, fax: 202/334-3471, http://www.nationalacademies.org/trb/idea)

TABLE OF CONTENTS

LIST OF FIGURES

LIST OF TABLES

1.0 BACKGROUND

1.1 Description of the DART

The Duomorph Asphalt Rheology Tester, also known as the DART, is a prototype system assembled to characterize asphalt binders. The DART system is comprised of the following components:

- A duomorph gage (also referred to as a DART gage)
- Two pre-soldered strain gages (attached on either side of the duomorph gage)
- Electrical leads (2 driving leads and 1 grounding lead)
- A signal conditioning unit
- A microcomputer with appropriate software to produce the drive signal and to log and analyze strain data from the DART
- A drive signal amplifier
- A temperature control chamber

The duomorph is a layered assembly of a metallic shim placed between two piezoelectric sheets. The overall thickness of the gage is on the order of half a millimeter. Piezoceramics belonging to the PZT-5A class, made from a composition of lead titanate-zirconate (PZT), were used in this study due to their superior characteristics over the temperature range of interest to asphalt binder testing. The different layers in the duomorph are held together by a fine layer of a special bonding agent. The manufacturer supplies the duomorph transducer elements as rectangular sheets that are later cut into circular disks. The overall thickness of the gages is on the order of one-half of a millimeter.

The exposed surfaces of the piezoceramic layers are finely coated with nickel to form electroded faces. Thin electrical leads are soldered to the surface of these electroded faces to facilitate the electrical excitation of the duomorph gage. Strain gages are attached to the center of each side of the duomorph. The poling axes of the piezoceramic sheets, which define their piezoelectric behavior, were asymmetrically arranged with respect to the neutral axis (i.e., both poling axes point in the same direction). This arrangement allows both faces to be driven simultaneously using the same signal source. Figure 1(a) and 1(b) present plan view and section sketches of the duomorph gage.

1.2 Principle of Operation

The piezoceramic layers function as electromechanical transducers capable of producing an electrical voltage when a mechanical deformation is applied to them and vice versa. When a voltage is applied to a PZT crystal it deforms, i.e., expands or contracts. In an electrically asymmetric duomorph gage, the poling axes of the two piezoceramic layers are oriented such that, when a voltage is applied across their electroded faces, one of the layers expands while the other contracts. This produces a bending action as indicated in the section view of the gage shown figure 2. It is clear from the figure that the maximum bending strain occurs at the center of the gage. Therefore, this is an ideal location for strain gaging. The magnitude of the bending strain at the gage center is directly proportional to the driving voltage. In fact, it has been observed in the laboratory that the amount of bending increases linearly with the applied voltage. While higher driving voltages are required to obtain cleaner signals particularly when the gage is embedded in cold asphalt, care must be taken to ensure that the driving voltage does not cross the depolarization limit of the duomorph. If this happens, the duomorph will loose its piezoelectric properties and will behave like an ordinary ceramic.

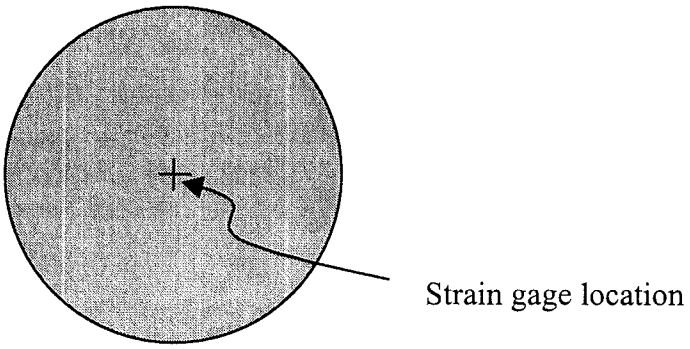

(a) Plan view

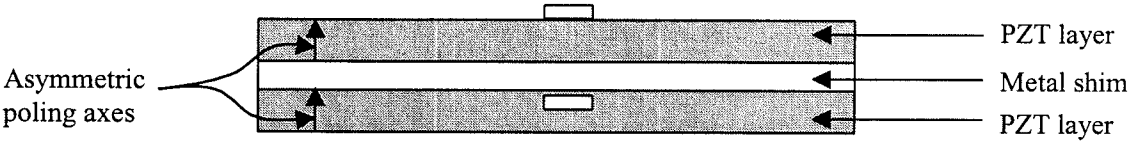

(b) Section view (not to scale)

Figure 1. The duomorph/DART gage.

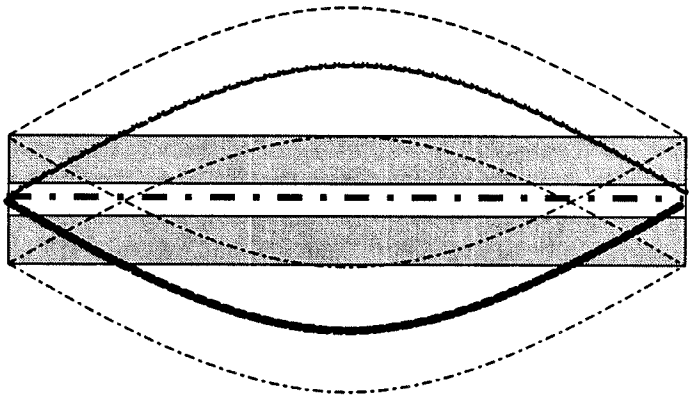

Figure 2. The duomorph in operation.

If the applied voltage signal is sinusoidal, the sensor vibrates sinusoidally at the same frequency as that of the input signal. When the duomorph gage is operated in air, the strain signal should exactly follow the trace of the driving voltage, i.e, the time lag or "signal shift" is zero. This provides a calibration point for analysis when the gage is embedded in asphalt. However, when the gage is embedded in a viscoelastic medium and vibrated, two significant changes occur to the signal. First, there will be a time lag induced in the response of the gage with respect to the applied driving voltage signal. Second, the peak strain will be reduced due to the confining effect of the stiffness of the surrounding medium. The signal shift along with the ratio of peak duomorph gage strains in air and in the medium, provide a means to compute the phase angle and complex modulus of the viscoelastic medium. Figure 3 presents a schematic of the duomorph operation, illustrating experimental determination of the signal shift. It is important to note here that the shift in the bending strain response is not the same as the phase angle, δ, of the asphalt binder. In fact, phase angle is just one of the parameters on which the signal shift is

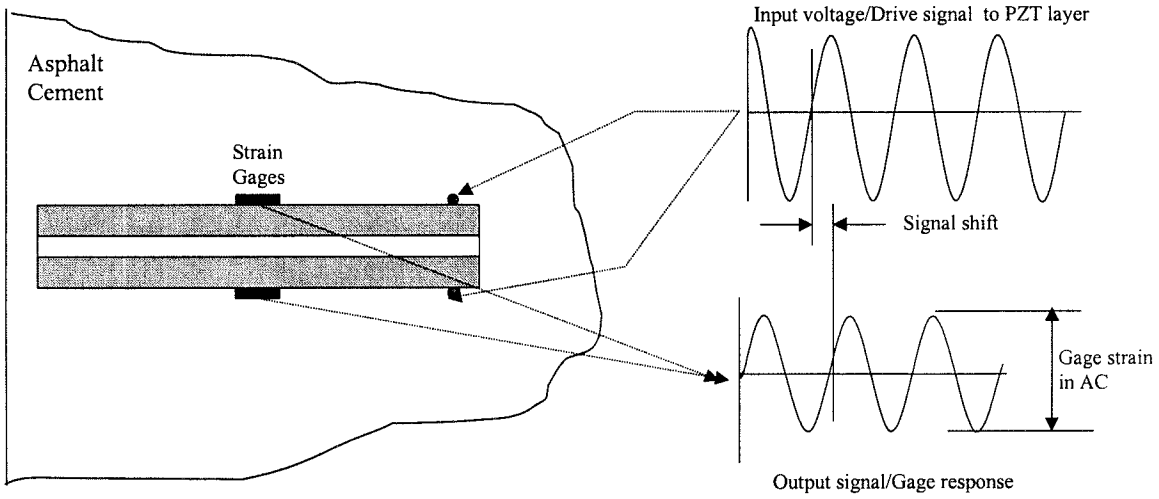

Figure 3. Schematic of duomorph operation illustrating gage strain and signal shift determination.

dependent upon. Other factors that influence this parameter include the stiffness of the surrounding medium and the geometric and material properties of the duomorph itself. In the current version of the DART, the strains at the gage center are recorded through strain gages mounted on the duomorph. The frequency of vibration can be set to match the rate of shear in the DSR testing, and can be continuously varied for a complete material characterization.

1.3 Prior Research

Preliminary motivation to investigate the DART as a tool to perform asphalt binder specification testing using the SHRP test protocol was obtained from the study of Briar et al (1, 2). In their study, Briar et al successfully investigated the duomorph as a permanently embedded sensor for long-term surveillance of the structural integrity of solid rocket propellant. The scope of their research covered fabrication of the duomorph sensor, development of an analytical data reduction scheme to determine the propellant's complex modulus from the duomorph response, and limited validation. Inasmuch as the work of Briar et al was successful, its application to testing asphalt binders required redevelopment of the entire process starting from instrumentation to validation. Some of the reasons necessitating this redevelopment are listed below:

- Several advancements have been made in the piezoelectric industry resulting in superior materials and manufacturing processes in the past twenty-five years. Further, the electronics required to drive the duomorph and the techniques to collect and analyze the data have also undergone significant improvements. The impact of these technological advances on the ability of the duomorph to characterize asphalt binders needs to be investigated.
- There were two parameters of interest in testing asphalt binders under the SHRP specification namely, the complex shear modulus (G*) and the phase angle (δ). The earlier work did not consider phase angle in its validation process as it was not a parameter of interest.
- The expected stiffness regime over which asphalt binders are to be tested varies over a wider range than was originally considered. The asphalt binder behavior over this regime ranges from near viscous to almost completely elastic. Consequently, a new data reduction scheme

eliminating some of the simplifying assumptions and incorporating more realistic material behavior needs to be developed.

The DART investigation was sponsored under an NCHRP-IDEA contract and proceeded in two phases. In phase I, the focus was on establishing the viability of the DART through a logical redevelopment of the "original" duomorph gage for application in asphalt rheology. Phase II dealt with a more comprehensive investigation resulting in the development of a prototype device.

The main experimental variables in phase I were the dimensions of the circular duomorph disks, instrumentation (including strain gage types and signal conditioning and amplification devices), methods employed for driving and grounding the duomorph gage, gage excitation voltages, and data reduction procedures. A user-friendly software interface was developed using the National Instruments software, LABVIEW, to facilitate gage excitation and data acquisition under this phase. The DART system that evolved at the end of phase I was the result of a continuous refinement process that spanned the entire length of the study and utilized the best methods and materials at the time. The feasibility of the system was evaluated by testing a reference asphalt binder at various temperatures, processing states (original versus PAV binder), frequencies, and strain levels. The raw data from the DART were examined, as part of the verification process, to investigate if the data agreed with engineering intuition. The raw data were then reduced using the procedure developed by Briar et al to determine shear moduli and phase angles. The computer program of Grosz (3) greatly facilitated this effort. The shear moduli and phase angles from the DART were compared with results obtained from the DSR and BBR devices for the same asphalt binders. Sensor ruggedness and durability were also under close scrutiny throughout the study. The following important conclusions were reached at the end of the phase 1 (4).

- Equipment has been assembled at a relatively low cost that shows considerable promise to test asphalt binders in accordance with the SHRP specifications.
- The DART gage and the associated electronics can withstand normal laboratory use for extended periods of time. This would suggest that it could also be used as a field QA/QC device where the conditions are more severe.
- The bending strains and phase shifts measured from the DART gage were highly repeatable.
- Tests conducted on the duomorph gage in air show a linear effect of increasing the driving or excitation voltage on the bending strain response. Further, it was also determined that the response is essentially constant with driving frequency within the range of interest to asphalt binder testing.
- Initial verification of the raw duomorph data from the DART embedded in asphalt indicates that the DART system is sensitive to changes in both the complex shear modulus and phase angle.
- The sensitivity of the gage to the changes in the surrounding medium seems to be a function of the ratio of the binder stiffness and the duomorph gage flexural rigidity. Initial testing indicates different DART gage sizes, construction, and/or materials will be required for testing asphalt binders over the entire stiffness regime.
- The G* values obtained from reducing the DART data for the reference asphalt were in excellent agreement with values determined from the DSR. The comparisons for the tank asphalt were made over a temperature range of 5°C to 60°C. Comparisons for the PAV aged asphalt were made at 22°C and 30°C. The data was reduced using schemes developed as part of the study by Briar et al,
- The G* values from the DART at low temperatures (below 0°C) support the argument that

the DART can obviate the need for individual pieces of equipment for different temperature ranges of testing. However, a refinement of sensor electronics and a proper matching of the flexural rigidity of the duomorph disk with the asphalt binder stiffnesses at these temperatures might need to be undertaken for obtaining more meaningful data.

Some limitations of the DART noted at the end of phase 1 study are listed below:

- While moderate success was achieved in determining phase angles at intermediate temperatures for PAV binders, the results at higher temperatures on unaged binders were unacceptable.
- There appears to be a limiting value of the asphalt stiffness to duomorph flexural rigidity ratio beyond which the DART is not sensitive to the changes in properties of the asphalt medium and operates as though it were in air. This occurs at the higher asphalt temperatures where asphalt is close to viscous behavior.
- The data reduction process developed by Briar et al is relatively tedious and is based on assumptions that need to be verified for the sample sizes and materials used in this study.

1.4 Objectives of Phase II Study

Some of the limitations noted at the end of phase I study were addressed as part of the work effort in this phase of the study. The main goal of the phase II study was to formalize the procedure for characterizing the asphalt binders leading to the development of a fully functional DART system. In order to accomplish this objective, the following tasks will need to be undertaken.

1. Standardization of duomorph gage dimensions and sample size.
2. Development of a theoretical analysis procedure to predict the DART gage response in air as well as in the asphalt cement specimen. This procedure should be capable of describing the physical viscoelasticity problem accurately.
3. Perform appropriate verification of the theoretical model.
4. Using the analytical scheme developed, conduct a parametric study over the typical ranges of asphalt cement complex shear moduli (G^*) and phase angles (δ) to develop a database of laboratory measurable duomorph responses.
5. Correlate the duomorph responses in the database to the assumed asphalt properties to develop a new data reduction scheme. Validate the data reduction procedure by testing reference asphalts.
6. Provide final recommendations.

In the conduct of this Phase II study, the research deals primarily with items 1 and 2. These items will be discussed at length in the following sections and represent, the development of an analytical tool to model the duomorph behavior which is central to the success of the DART system.

2.0 GAGE DESIGN AND OPERATIONAL ISSUES

2.1 Duomorph Dimensions and Flexural Rigidity

In phase I, gage diameters were varied at three levels (19 mm, 25 mm, and 50 mm). The thickness of piezoelectric layer had to be held constant at 0.19 mm due to manufacturing restrictions. Only stainless steel based metallic backing was used in the duomorph for the phase I study. The thickness of the steel shim backing was varied at two levels—0.13 and 0.20 mm. The overall gage thicknesses thus varied from 0.51 mm to 0.58 mm.

In phase II, thinner duomorph gages with a brass metallic shim were investigated along with the stainless steel shim-based gages. The objective behind introducing a thinner shim or a softer metal was to increase the gage sensitivity by decreasing the flexural rigidity. It was empirically observed in the phase I study that a more sensitive gage would be required at the elevated testing temperatures when the gage is embedded in asphalt. Table 1 presents a list of the various DART gages considered in this study (both phases) along with their respective flexural rigidities.

Table 1. Dimensions and flexural rigidities of the duomorphs assembled.

Duomorph Description		Thickness, mm		Diameter, mm	Flexural Rigidity, D N-mm
Name	Poling Axis Orientation	PZT	Steel		
DART # 1A	Symmetric/Asymmetric	0.1905	0.2032	25.4	759.69
DART # 2B	Symmetric/Asymmetric	0.1905	0.1270	19.05	1228.44
DART # 3A	Symmetric	0.1905	0.1016	50.8	641.69
DART # 4A	Symmetric/Asymmetric	0.1905	0.1016	25.4	641.69
DART # 5C	Symmetric/Asymmetric	0.1905	0.0	19.05	308.64

The flexural rigidity in table 1 was computed using equation (1):

$$D = \frac{E_z h^3}{12(1-\nu^2)}\left[1+\left(\frac{E_m}{E_z}-1\right)\left(\frac{h_m}{h}\right)^3\right] \qquad \text{Eq. 1}$$

where,

D	=	plate flexural rigidity given by the expression
E_z	=	modulus of the PZT wafer
E_m	=	modulus of the metal shim
h_m	=	thickness of metal shim
h	=	overall thickness of the duomorph

2.2 Strain Gages and Electrical Leads

In phase II, the type of strain gages, leads, bonding agents used and the methods employed in attaching strain gages to the duomorph disks were finalized to provide consistency and improve durability of the DART. Strain gages from Micro Measurements, Inc.,of the type EA-06-125AC-350 with a gage length of 3.1 mm were adopted. These gages come with pre-soldered leads. The M-Bond 200™ bonding agent with excellent characteristics over the range of temperatures of interest of asphalt binder testing was employed to attach the strain gages to the duomorph disk. An interesting observation noted in investigating the optimal techniques to affix strain gages was that marking the duomorph surface with lead-based markers causes a loss of charge from the areas with the markings leading to an undesirable increase in the amount of current drawn. Therefore, markings were made with a fine felt-tipped pen. A 16-guage single conductor lead was soldered on to each of the two electroded faces of the duomorph to carry the electrical charge produced by the piezo-driving subassembly. A 16-guage multiconductor lead was used to electrically ground the duomorph.

Semiconductor strain gages were also experimented with for the extremely low temperature tests to obtain a better strain output. However, the extremely delicate nature of these gages and their cost precluded their general use in this research.

2.3 Piezo Driving and Grounding Issues

The poling axes of the piezoceramic layers in the phase I study were symmetric about the neutral axis of disk as shown in figure 4 and there was no independent ground available. This arrangement allows only one face of the duomorph to be driven with respect to the other face, which is grounded resulting in an inefficient design since only one-half of the net piezoelectric potential is being utilized. If both faces in such a design are to be driven simultaneously an independent ground source needs to be established. This was accomplished by introducing a small grounding tab while cutting the circular duomorph disk from the square sheets supplied by the manufacturer. The tab is cut in a triangular shape and is sized to have just enough space to solder a ground lead on to it. The presence of this tab is not expected to cause significant changes to the duomorph's response profile and can be ignored in the analysis. The piezoceramic material on either sides of the tab was filed until the metal shim was exposed. A fine lead was soldered on to this metallic tab and was used to provide the electrical ground for the duomorph. The circular disk with the grounding tab is shown in figure 5. Further modifications to the design included arranging the piezoelectric layers with their poling axes asymmetrically placed about the neutral axis. This arrangement allows the both the faces of the duomorph to be driven simultaneously with a voltage signal of like polarity effectively doubling the strain output.

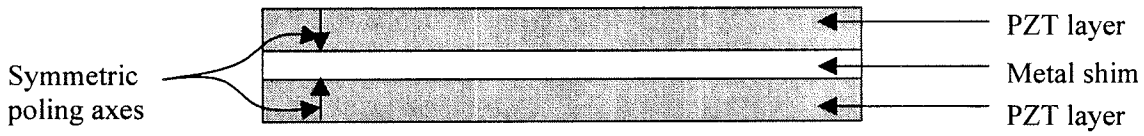

Figure 4. Duomorph gage with symmetrically arranged poling axes.

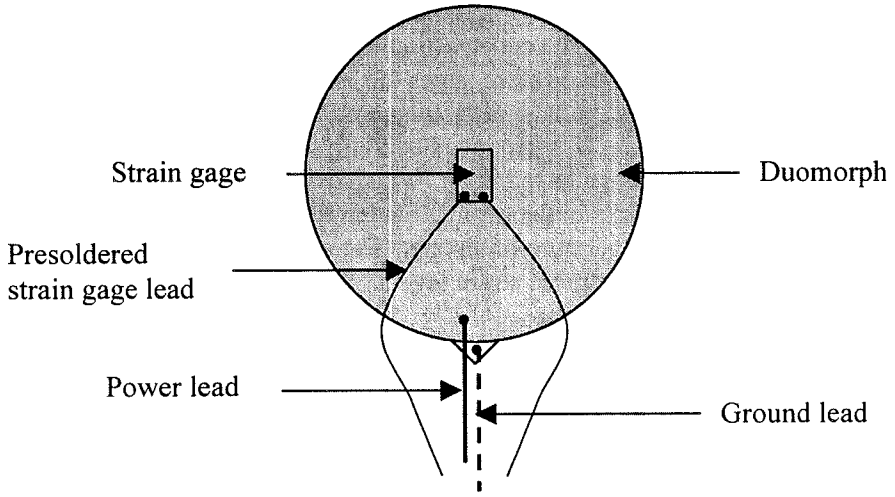

Figure 5. Duomorph gage showing details of grounding tab and lead connections .

When the asphalt is very stiff, e.g., at cold temperatures, the confining effect on the duomorph is very high, resulting in a lower strain at the gage center. A very low strain signal is hard to interpret accurately especially when the amplitude of the signal is such that the noise inherent to

the system can obfuscate it. In other words, the signal-to-noise ratio is a definite concern at the lower temperatures where the asphalt binder is very stiff. Obviously, a higher AC driving voltage is required to obtain a clean signal at these temperatures. Experimental trials revealed that the duomorph strain response varies linearly with the driving voltage, i.e., if the driving voltage is increased from 30 V_{p-p} to 120 V_{p-p}, the flexural strain of the duomorph gage center essentially quadruples. This phenomenon allows for a lower driving voltage when the asphalt is relatively "soft" and a higher driving voltage when it is hard. However, there is a capping voltage beyond which if the duomorph gage is driven, the piezoceramic crystals will reorient themselves in a way that the piezoelectric effect is lost and PZT layer will behave like a normal ceramic. For the purposes of this study a maximum, peak-to-peak driving voltage of 120 V_{p-p} was adopted. The manufacturer limitation on the maximum drive voltage for the materials employed in this study was 180 V_{p-p}.

2.4 Signal Conditioning and Amplification

Another important component of the DART assembly is the signal conditioning and amplification unit. This is the perhaps the bulkiest of all components assembled in the prototype. Initial trials with Analog Devices 5B series backplane and miniature strain gage input modules proved unsuccessful due the limited signal amplification available with this setup. However, more recent developments in this area remain to be pursued. At the lower temperatures, the strain output from the duomorph is very small and will require amplifications of up to x2000 for the given driving voltages and sensitivities of the strain gages used. A Measurements Group® Vishay 2000 unit is currently being used in the prototype to provide signal amplification. The Vishay unit, which has two internal 350-ohm resistance gages, completes the Wheatstone bridge circuit along with the two strain gages affixed to the duomorph. The bridge excitation was varied from 10 to 15 VDC to determine the optimal value for the various asphalt stiffnesses considered.

2.5 Summary—Standardized Duomorph Gage and Operation

The 25-mm duomorph gage with a total thickness of 0.5 mm (piezoceramic sheet thickness = 0.19 mm and stainless steel shim thickness = 0.127 mm) with attached Micro Measurements EA-06-125AC-350 strain gages was adopted as the standard for phase II testing. The primary factors governing this decision are the ease of the construction of this gage from raw materials and its relatively large range of sensitivity (brass shim gages did not produce any greater sensitivity). The gage was driven at 120 V_{p-p} AC voltage at all temperatures and the DC excitation provided in the strain gage bridge was 15 VDC. This produced bending strains in the order of 0.05 percent at the center of the duomorph gage when tested in air (which essentially represents the maximum strain encountered). The strain levels in the asphalt binder are expected to be lower than or equal to this value, depending on the temperature of testing. The asphalt cement is expected to be within the linear viscoelastic range at these strain levels.

Additionally, a Vishay signal conditioning unit, a LABVIEW virtual instrumentation software interface, an x15 piezo voltage signal amplifier, a portable temperature control chamber, and a microcomputer complete the list of components assembled for the DART operation.

2.6 Asphalt Specimen Size and Gage Embedment

According to Briar et al, when the duomorph gage is embedded at the center of a cube of asphalt material whose side length is greater than twice sensor diameter, edge effects on the strain response of the gage are negligible. It was conjectured as part of this study that the specimen size in the direction of motion of the duomorph gage while it is in operation, has the most influence on its response due to the material perturbation in this direction. The specimen size in the directions

orthogonal to this direction will not have a significant impact on the response. Based on this assumption, cylindrical asphalt specimens with a diameter at least twice the size of the duomorph gage and a height up to100-mm were chosen for testing. For PAV samples a cylinder of 50 mm was used due to the difficulty anticipated in processing the amount of asphalt required for a 100-mm high cylindrical specimen. The duomorph gage is lowered into the heated asphalt cement vertically such that it is centrally located in the specimen. It is important to adhere to locating the gage as centrally as possible in the specimen since this positioning is assumed in developing the data reduction procedure. In order to facilitate accurate embedment of the gage, a guide sleeve shown in figure 6 was manufactured from a metallic channel section. The bottom of guide sleeve rests on the bottom of the container holding the asphalt specimen and the duomorph is positioned as shown in figure 6. In addition to facilitating gage placement, the sleeve also helps avoid hauling the gage out of the asphalt specimen by directly pulling on the lead wires.

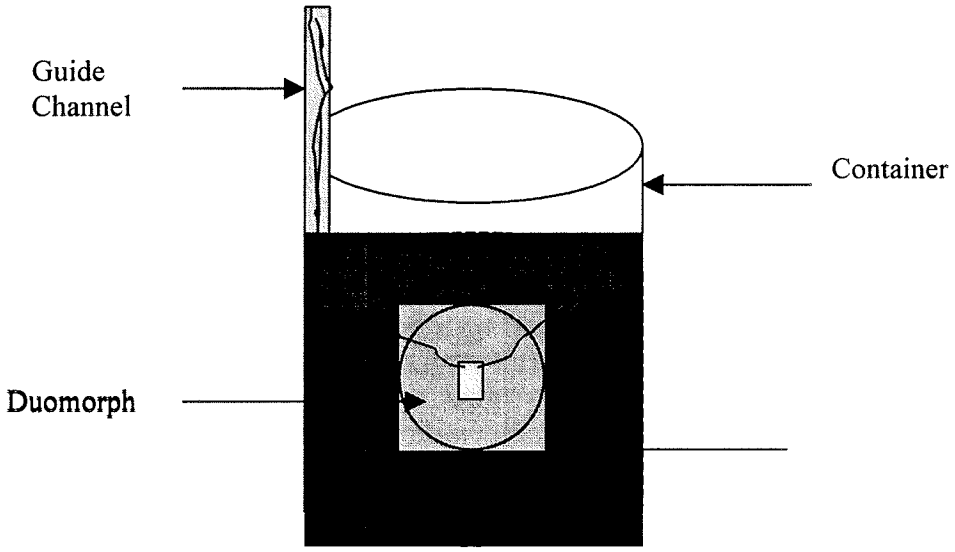

Figure 6. Duomorph embedment with the help of a guide channel.

3.0 DART MEASUREMENTS

3.1 Repeatability of the DART Output

In this round of DART testing, the consistency with which the duomorph collects data was tested. The ADART#1c gage was used to perform testing over a wide range of temperatures and frequencies. The repeatability of the gage output, i.e., the bending strain at the center of the gage and the signal shift, was studied both in air and in asphalt. The testing sequence is as follows:

Step 1: Heat the asphalt specimen to about 140°C for about 5 minutes to allow the DART gage to be inserted.
Step 2: Insert the ADART#1c gage with the help of the guide channel into the asphalt specimen taking care that the gage is as close to the center of the specimen as possible.
Step 3: Place the specimen with the gage into a temperature control chamber.
Step 4: Bring the specimen to the desired test temperature and take 10 observations for each frequency of interest.
Step 5: Repeat step 4 for all test temperatures of interest.

The test temperatures adopted for this study were 5°C, 10°C, 20°C, 40°C, and 55°C. At each temperature, the asphalt specimen was tested at 0.1, 1, 1.59, 10, 30, and 100 Hz. This type of testing is aimed at characterizing the variability of the DART gage output during a single setting of frequency and temperature sweep analysis of an asphalt binder. The primary source of variability in such a study is from the changes in electrical signals in the sensor electronics at a given test point. Tables 2 and 3 summarize the findings of this study at a test frequency of 1.59 Hz.

Table 2. Repeatability analysis of bending strain output at the duomorph gage center at a test frequency of 1.59 Hz.

Obs.	Peak-to-Peak Gage Stain in Air, Volts	Gage Strain Output in Asphalt, Volts				
		5°C	10°C	20°C	40°C	55°C
1	7.75	0.270	1.016	3.656	7.219	7.688
2	7.75	0.270	0.962	3.656	7.312	7.500
3	7.75	0.276	0.975	3.656	7.250	7.625
4	7.75	0.281	0.975	3.656	6.969	7.625
5	7.525	0.274	0.968	3.594	7.000	7.500
6	7.75	0.272	0.906	3.500	6.844	7.375
7	7.75	0.274	0.989	3.500	6.906	7.438
8	7.75	0.278	1.016	3.406	6.875	7.312
9	7.75	0.270	0.984	3.375	7.031	7.435
10	7.75	0.268	0.937	3.500	7.125	7.500
Mean	*7.728*	*0.274*	*0.973*	*3.550*	*7.053*	*7.450*
Std. Dev.	*0.071*	*0.004*	*0.034*	*0.108*	*0.165*	*0.118*
COV	*0.92%*	*1.44%*	*3.46%*	*3.05%*	*2.34%*	*1.58%*

Table 3. Repeatability analysis of signal shift output at the duomorph gage center at a test frequency of 1.59 Hz.

Obs. No.	Signal Shift in Air, msec	Signal Shift Output in Asphalt, msec				
		5°C	10°C	20°C	40°C	55°C
1	28	394.9	250	110	34	30
2	28	390.9	260	110	34	30
3	28	388.9	260	104	34	30
4	28	392.9	256	106	34	30
5	28	396.9	256	108	38	30
6	28	392.9	274	112	36	30
7	26	390.9	254	108	34	28
8	28	396.9	244	112	36	28
9	28	394.9	256	112	36	28
10	28	394.9	262	114	36	26
Mean	*27.8*	*393.5*	*257.2*	*109.6*	*35.2*	*29*
Std. Dev.	*0.063*	*2.67*	*7.90*	*3.10*	*1.40*	*1.41*
COV	*2.28%*	*0.68%*	*3.07%*	*2.83%*	*3.97%*	*4.88%*

The mean coefficient of variation (COV) of the duomorph strain measurements in asphalt averaged over the entire range of test temperatures is 2.3 percent and the mean standard deviation is 0.072 V from table 2. Likewise, the mean COV of the duomorph signal shift measurements is 3.1 percent and the mean standard deviation is 3.3 msec from table 3. The readings when the

DART is operated in air are even more consistent as evidenced by the data in tables 2 and 3. It is clear from this testing that that the duomorph is capable of providing highly repeatable outputs.

Note that in the all the testing reported above, the DART gage, once embedded in the asphalt, remained there throughout. Further only one DART gage was used in testing. Therefore, the repeatability study above does not capture the effect of variability caused by factors such as:

1. Daily variations in the electric signal used to drive the dumorph.
2. Slight changes in dimensions (thicknesses and diameters) of different duomorph gages when they are manufactured from different lots of raw materials.
3. Slight misalignment of strain gages during application.
4. Change in duomorph characteristics with age.
5. Off-center placement of the duomorph gage in the asphalt specimen.

All the factors noted above, with the exception of the last one, impact the strain response of the duomorph in air as well as in asphalt equally. Hence, the ratio of the strain in asphalt and in air (strain ratio) remains unaltered as long as both the readings are taken at closely spaced intervals. Recall that the strain ratio is the primary parameter of interest in the DART analysis. In general, it is recommended that the DART gage output in air be recorded just prior to starting a sequence of tests in asphalt to provide the reference point used in calculations.

Any variability produced by misalignment of the DART gage with respect to the center of the specimen is however uncalibratable. The primary concern here is that if the gage gets too close to the walls of the container holding the asphalt specimen, the assumption made in the data reduction process that the gage is surrounded by significantly large amount of material on all sides is violated. The changed boundary conditions might lead to a response far different than what is representative of the material being tested. Although, the guide sleeve, with the help of which the DART gage is placed in the specimen, limits large-scale misalignments, it is worthwhile to study the variability associated with this factor. A limited testing program was therefore undertaken using the ADART#1c gage. A frequency of 1.59 Hz was used and the asphalt specimen was tested at two temperatures 20 °C and 55°C. At each temperature 5 observations of the gage response were collected. The DART gage was removed after each observation and reinserted into the asphalt specimen before the next observation was taken, all the while ensuring that the gage position is as close to the center of the specimen as possible. Although in reality it is highly unlikely and also undesirable to remove the gage between successive readings in a temperature sweep analysis, this study undertaken is aimed at simulating the variability associated with asphalt testing performed over several days on the same specimen. The results of this study are reported in table 4.

Table 4. Repeatability analysis of bending strain and signal shift with repeated removal and reinsertion of the duomorph gage from the asphalt specimen.

Obs. No.	Duomorph Strain Output in Asphalt, Volts		Duomorph Signal Shift Output in Asphalt, msec	
	Specimen Temp= 20°C	Specimen Temp = 55°C	Specimen Temp = 20°C	Specimen Temp = 55°C
1	3.656	7.688	110	30
2	3.560	7.400	114	30
3	3.452	7.625	104	26
4	3.650	7.635	106	30
5	3.340	7.325	104	28
Mean	*3.532*	*7.535*	*107.600*	*28.800*
Std. Dev.	*0.121*	*0.144*	*3.878*	*1.600*
COV	*3.43*	*1.91*	*3.60*	*5.56*

The average standard deviation and COV of the strain output for the two temperatures studied are 0.133 V and 2.67 percent, respectively. Likewise, the average standard deviation and COV of the signal shift output are 2.74 msec and 4.58 percent, respectively. Note that the corresponding values from table 2 for the strain output were 0.11 V and 2.3 percent and for the signal shift output from table 3 were 2.25 msec and 3.8 percent, respectively.

The combined variance of the duomorph tests for these two temperatures can therefore be determined using the sum of the individual variances as follows:

$$\sigma^2_{combined} = \sigma^2_{testing\,1} + \sigma^2_{testing\,2} \qquad \text{Eq. 2}$$

The standard deviation can be determined by simply taking a square root of the variance. Using this approach, the standard deviation of the strain output after taking into account all possible forms of testing variability is 0.173 V. The standard deviation of the signal shift was estimated to be 3.55 msec. Both these estimates of variability are within acceptable ranges. Therefore it can be concluded that, under a single operator environment, the repeatability of the duomorph data output is highly repeatable.

3.2 Sensitivity of the DART Gage

The viability of the DART for characterizing asphalt binders can be determined by verifying its sensitivity to changes to the primary parameters of interest—G* and δ. Such verification is intended to illustrate whether the duomorph responses follow engineering intuition in a manner amenable to analytical interpretation. If this criterion is not met, the conceptual model may be unsatisfactory and need to be addressed before any further testing is conducted. For example, as part of the phase I study it was established that at any given frequency, as the test temperature is lowered, the strain response from the duomorph embedded in asphalt reduces due to the increasing stiffness of the asphalt. The change in response is smooth and is void of any discontinuities. Similarly, it was shown during testing that as the test temperature increases the lag between the duomorph strain response and drive signal (signal shift) tends to zero degrees, i.e., at high temperatures where the asphalt is very soft the duomorph gage response is similar to that seen in air. These trends are consistent with the conceptual model of the duomorph response and demonstrate that the development of correlations between asphalt properties and duomorph gage responses can be accomplished. However, since the observations on the gage sensitivity

established in phase I were based on limited testing, a more detailed investigation in phase II. The findings of this investigation are presented below.

Three original or tank asphalt binders were chosen for the sensitivity analysis in phase II. Based on viscosity grading, these asphalts represented neat AC-10 and AC-40 viscosity graded binders. An AC-20 tank asphalt processed in the pressure aging vessel (PAV) provided an additional specimen to perform the sensitivity analysis.

As a first step, these asphalts were characterized in the laboratory using a Dynamic Shear Rheometer (DSR) to assess their properties. Each asphalt cement was tested in the constant stress mode at a variety of temperatures (from 5 °C to 60°C) and test frequencies (0.1 to 100 Hz). The testing was done in accordance with the SHRP binder protocol for DSR testing. The variation of the asphalt properties of interest, i.e., G* and δ for each of the binders considered is shown in figures 7 and 8. The properties shown in the figures were measured at a frequency of 1.59 Hz (10 rad/s).

Upon completion of the DSR testing, the asphalt binders were poured into cylindrical containers to form asphalt specimens of the desired dimensions to allow DART testing. The specimens were tested in succession with the ADART#1c gage (see table 1 for construction details of this gage). The testing sequence included heating the asphalt specimen to about 140 °C for a short period of time, inserting the DART gage assembly, placing the specimen into a temperature control

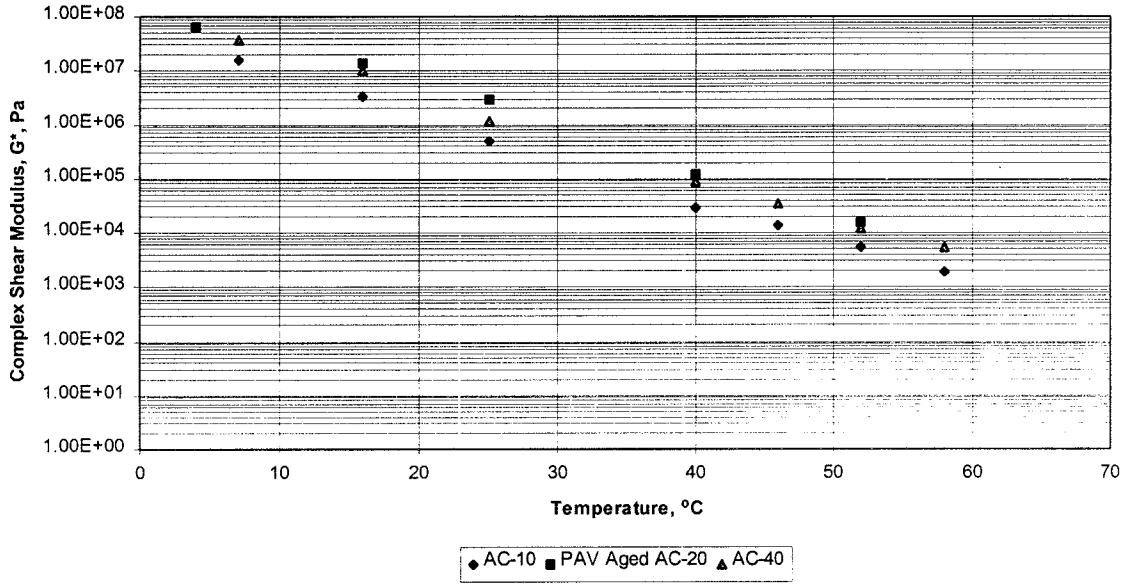

Figure 7. Variation of asphalt complex shear modulus G* with temperature.

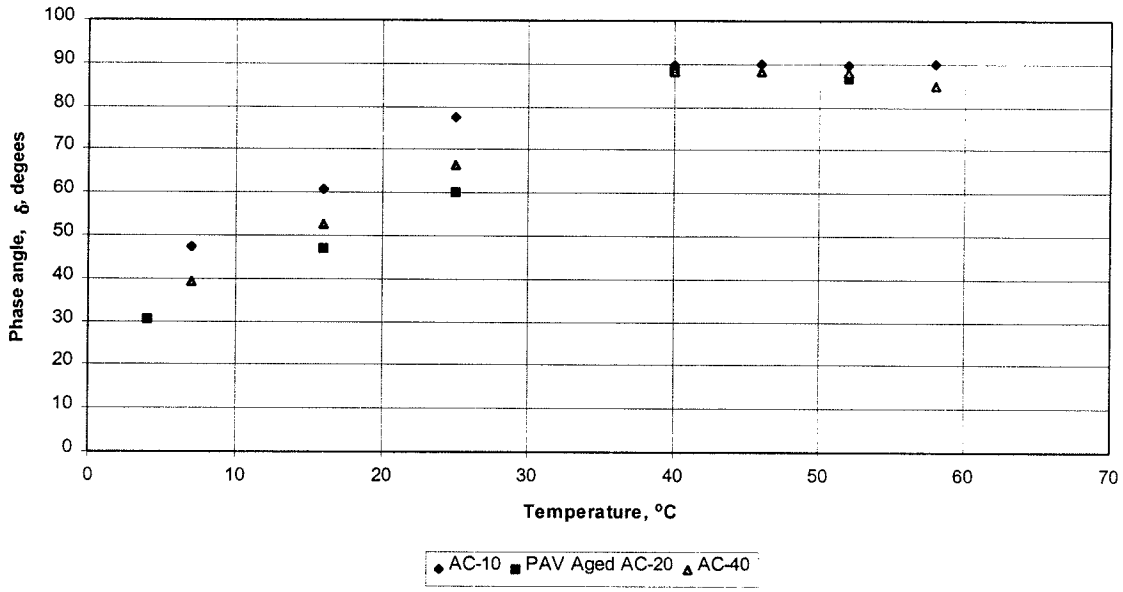

Figure 8. Variation of asphalt cement phase angle with temperature.

chamber, and performing the frequency sweep tests. This routine was repeated for a range of temperatures for each of the asphalt specimens.

Figures 9 and 10 summarize the responses obtained from DART gage ADART#1c at a frequency of 1.59 Hz. In figure 10, the strain ratio represents the ratio obtained by dividing the strain measured from the DART gage in asphalt binder with the strain in air. In figure 11, signal shift is the lag in DART gage response with respect to the applied forcing function (120 V_{p-p} AC voltage @ 1.59 Hz frequency). The following observations can be made from the figures:

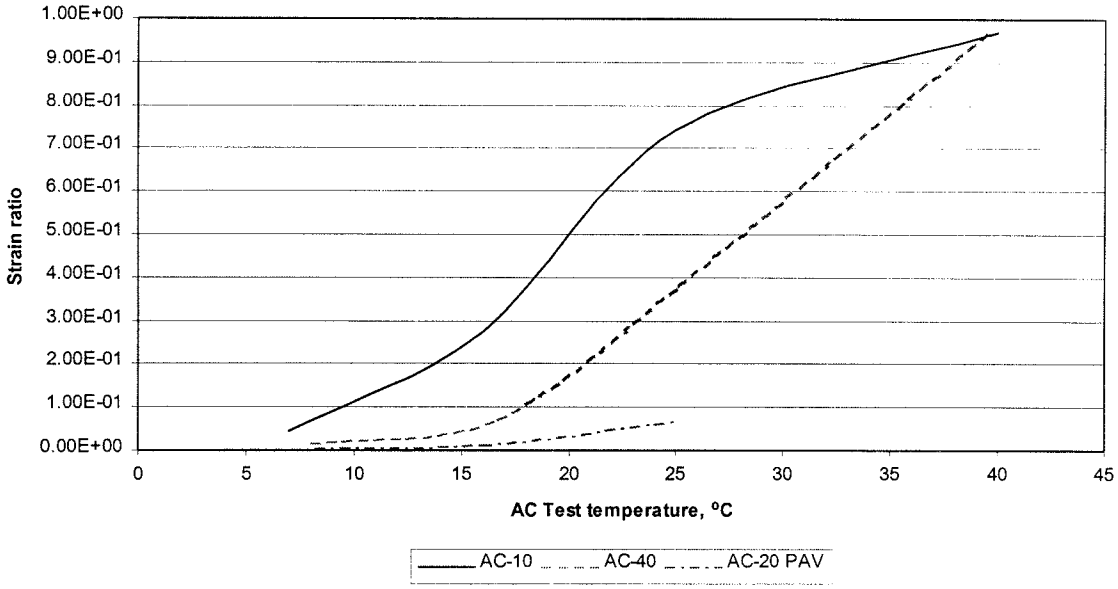

Figure 9. Variation in duomorph strain ratio ($e_{asphalt}/e_{air}$) with temperature.

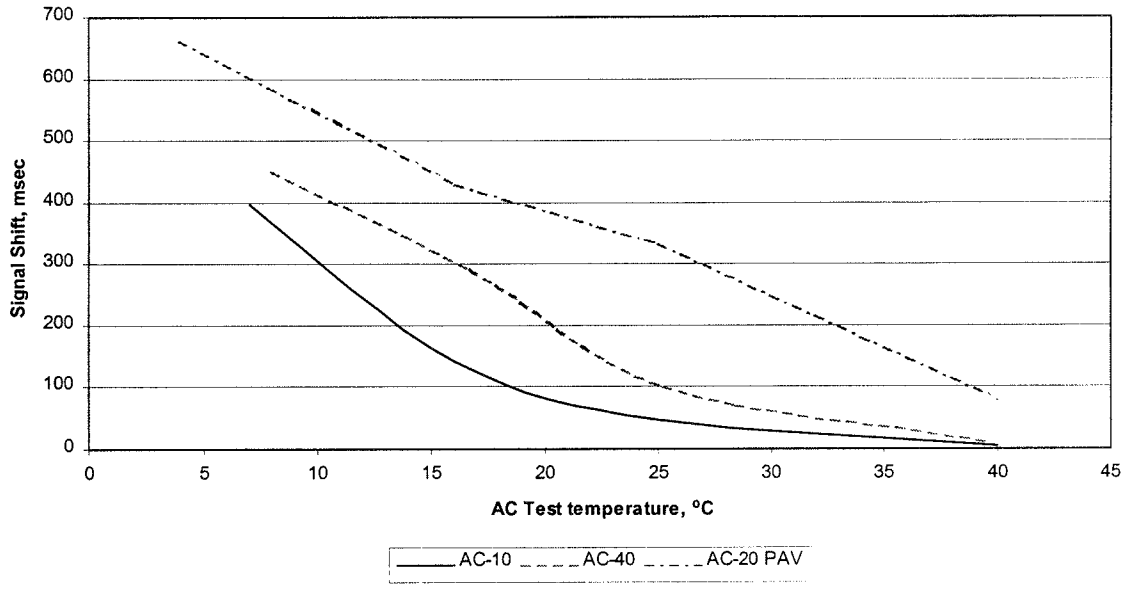

Figure 10. Variation in shift angle with temperature.

- The strain ratio increases as the temperature of the asphalt specimens increases or alternately as the stiffness decreases. The signal shift decreases with increase in specimen temperature. These trends are consistent across the asphalt specimens tested.
- At any given temperature, when the asphalt specimens are arranged in the order of decreasing strain ratios, the following sequence is observed: AC-10, AC-40, AC-20 PAV. This shows that the duomorph gage is appropriately sensitive to changes in the mechanical properties of the binder.
- The increase in the strain ratio and the decrease in the signal shift with temperature appear to follow an S-shaped curve. The strain ratio and shift angle curves when taken together for a given asphalt binder form a unique signature for the asphalt binder being tested.
- The strain ratio versus temperature curve reaches its maximum value of 1.0 and continues to remain there beyond a certain cut-off temperature (a strain ratio of 1.0 implies that duomorph strain in the asphalt specimen is the same as that in air). This cut-off temperature increases with increasing viscosity grade or processing age of the asphalt and represents a limiting stiffness for the duomorph test.

Several important conclusions can be reached based on the observations noted above. First, the duomorph gage is capable of producing an output unique to a given binder type. This observation lends itself well to correlation studies relating the gage response to the material properties of the medium. Such a study based on finite element analysis will be discussed immediately following this section. The next important conclusion is based on the asymptotic behavior of the strain ratio versus temperature curves shown in figure 9 at the higher temperatures. This observation suggests that there are limitations to the effectiveness of the ADART#1c gage. It is surmised here that the cut-off temperature or stiffness beyond which the gage is not effective in providing a unique strain signal is a function of the mechanical properties of the asphalt binder it is embedded in as well as the properties of the gage itself. A non-dimensional stiffness parameter M' was used to represent the continuum to gage stiffness. This parameter is expressed as below:

$$M' = \frac{E' a^3}{D} \qquad \text{Eq. 3}$$

where,

a	=	plate flexural rigidity given by the expression
E'	=	real part of the complex shear modulus of asphalt, N/mm^2
D	=	flexural rigidity of the duomorph gage, N-mm
h_m	=	diameter of the duomorph gage, mm

This parameter was plotted against the strain ratios determined from the AC-10 and the AC-40 binders in figures 11 and 12, respectively. A sharp inflexion point can be observed in the strain ratios when the M' value reaches $5*10^{-4}$ for the AC-10 binder and $6.5*10^{-3}$ for the AC-40 binder respectively. To the left of this inflexion point the duomorph gage produces more or less a constant strain ratio. For the given tank asphalt binder stiffnesses and the ADART#1c gage flexural rigidity, this means that the gage tends to lose its sensitivity around 40 °C to 45 °C. This can be taken as a limiting stiffness ratio beyond which this duomorph is not sensitive enough to provide valid data.

Equation 3 suggests that, for a given asphalt stiffness E', using a gage with a D value smaller than the ADART #1c gage increases the M' which in turn increases the sensitivity of the duomorph. Consequently, matching the flexural rigidity of the gage to the real part of the continuum complex modulus is of paramount importance in DART testing. This, when accomplished, could lead to the use of duomorph gages with varying flexural rigidities to test binders in different regions of the stiffness spectrum. Recall that the flexural rigidity of a gage is a function of its material properties as well as the dimensions. However, changing a certain set of parameters will be more efficient than changing others. For example, considering that the duomorph gage is already extremely thin, reducing the thickness, while theoretically reducing the flexural rigidity of the gage might make the production of the gages very expensive or impractical. On the other hand, the use of piezoplastics in place of piezoceramics can be a viable option. Piezoplastics have

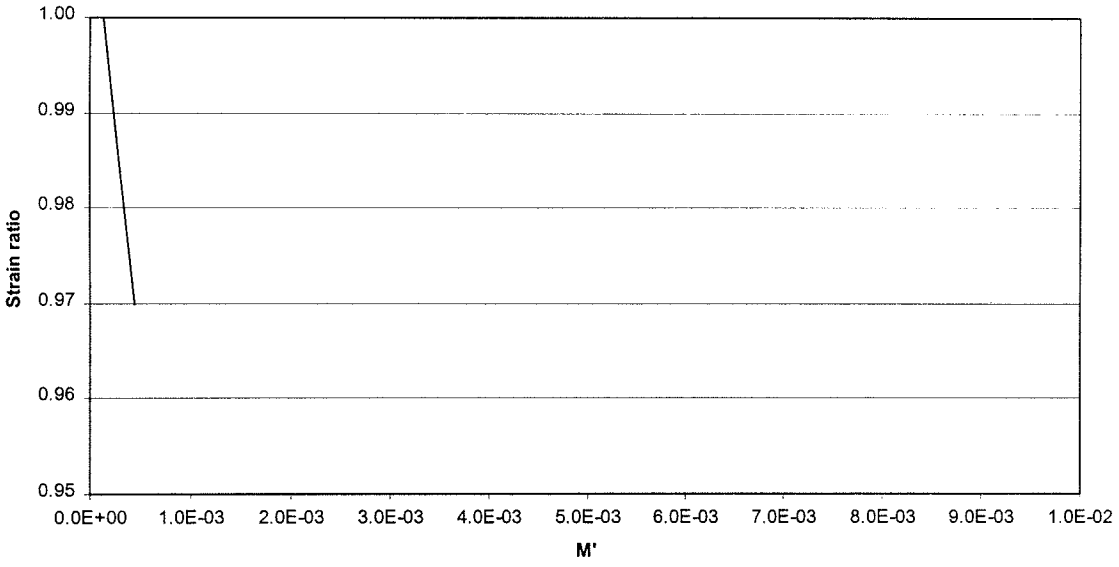

Figure 11. Strain ratio versus non-dimensional stiffness M' for the AC-10 asphalt binder.

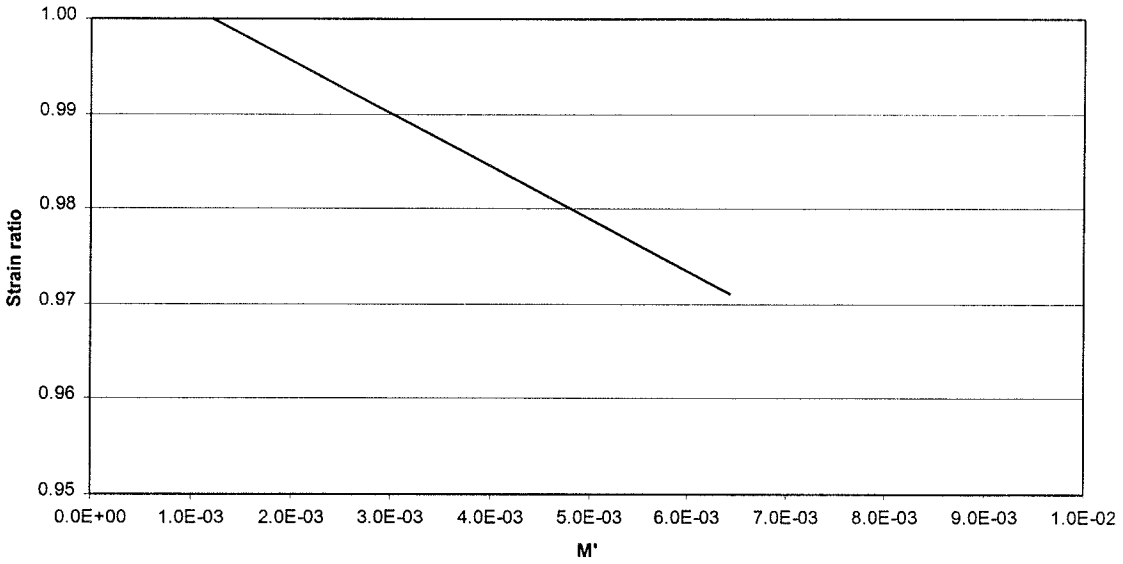

Figure 12. Strain ratio versus non-dimensional stiffness M' for the AC-40 asphalt binder.

lower stiffnesses and are capable of producing higher strains which are beneficial when testing low stiffness materials. The availability of an appropriate analytical model allows these options to be investigated without the time of an experimental investigation.

4.0 FINITE ELEMENT BASED THEORETICAL INVESTIGATION

A theoretical investigation of the duomorph was undertaken using the finite element approach. There were multiple objectives for this investigation, some of which are listed below:

- To develop an analytical model that appropriately describes the physical problem at hand. With the help of this model, a new data reduction scheme will be developed that will determine asphalt binder properties from the measured responses of the duomorph gage.
- To help optimize gage design obviating the need to perform laborious and expensive laboratory investigations. Recall that it was pointed out in the preceding discussion that duomorph gages with different flexural rigidities might be needed to for various stiffness regimes of the asphalt specimens. Flexural rigidities can be altered by varying either the mechanical properties or the dimensions (diameter or thickness) of the gage. This trial and error process can be greatly facilitated by finite element simulations.
- To support future development of the duomorph by modeling other gage shapes and materials that can lead to lower production costs.

The main focus of the discussion here will be on the development of a finite element model to simulate the responses of the ADART#1c gage in air and in asphalt. The main reason for the selection of this duomorph was that it produced consistent laboratory results. The inputs to the model include material properties of the gage obtained from the manufacturer, assumed properties of the asphalt binder, and the magnitude of the driving force. The primary outputs are the bending strain response at the center of the gage and the shift in the gage response with respect to the drive signal. The finite element responses will be validated through laboratory measured ADART#1c responses thus establishing an analytical model to simulate the gage response. An investigation will also be performed to examine the requirements necessary to extend the capabilities of the duomorph beyond what can be currently achieved in the laboratory.

4.1 Desired Capabilities of the Modeling Tool

Generally speaking, the duomorph behavior in air as well as in asphalt can be fully analyzed using a finite element program with following features:

- A library of finite elements with two- and three-dimensional elements capable of approximating the quadratic displacement field anticipated when the duomorph flexes back and forth in response to the applied electrical voltage. The elements should be capable of degrees of freedom related to both stress/strain analysis as well as piezoelectric analysis.
- A materials library that includes capabilities to model elastic, viscoelastic, and piezoelectric material behavior.
- Ability to perform static, steady state dynamic, and transient dynamic analysis.
- Ability to couple piezoelectric, dynamic, and viscoelastic analyses.

The general-purpose finite element program ABAQUS™ contains most of the desired features and was chosen to perform the analyses. ABAQUS offers a huge database of rigorously tested elements (including piezoelectric elements), materials, and procedure libraries that could be used in the analysis of the duomorph. Using ABAQUS, a finite element model of the duomorph could be constructed to varying degrees of complexity. Many types of coupled problems can also be examined. However, some limitations in the current version of the ABAQUS program were noted with regard to solving the duomorph problem. These include the inability of ABAQUS to

model nonlinear piezoelectric materials and to perform piezoelectric analysis coupled with transient dynamic analysis. This later limitation limits the ability of the program to perform the duomorph analysis in asphalt using time-domain viscoelastic inputs. These shortcomings however did not hamper the overall analysis objectives of the study seriously since, for example, the piezoceramic duomorph gage is not expected to behave nonlinearly. Further, since the duomorph is expected to vibrate at a relatively low frequency (1.59 Hz) during binder testing, a steady state analysis is adequate to characterize the response and a transient dynamic analysis is not required.

4.2 Modeling the Duomorph Response

4.1.1 Key Analysis Assumption

Prior to developing a working finite element model of the duomorph, a simplifying assumption was made with regard to load definition. Strictly speaking, distributed or concentrated electrical charges applied to the electroded duomorph faces accurately define the loading of the duomorph. Although ABAQUS has the capability to apply this type of loading, the properties of the piezoceramic material, such as the piezoelectric stress or strain coefficient matrix and the dielectric coefficient matrix, that are required to support the analysis were difficult/impossible to obtain from either the manufacturer or published literature. The constitutive equation governing the mechanical behavior of the gage requires either the piezoelectric stress coefficient or strain coefficient matrix as input, whereas, the equation governing the electrical behavior requires a dielectric property matrix as input. A definition of the piezoelectric behavior in the most general condition (anisotropic behavior) requires 18 independent constants for the piezoelectric stress or strain coefficient matrix and 6 constants for the dielectric matrix. This data is extremely difficult to obtain.

In order to overcome this problem, the approach of Briar et al. was consulted. In their approach, Briar et al showed that, within the context of classical plate theory, the effect of applying a voltage to the gage on the bending strain and deflection is same as applying a concentrated moment around the gage's periphery. Recognizing that the duomorph in bending is similar to a thin plate in bending, this equivalence can be taken advantage of without much loss of generality. The equivalence between the electrical and mechanical loads is shown in figure 13 and transforms the problem from a piezoelectric domain to a mechanical domain. Several other advantages brought about by this correspondence include reduced model complexity due to simplification of materials inputs and reduced computational time.

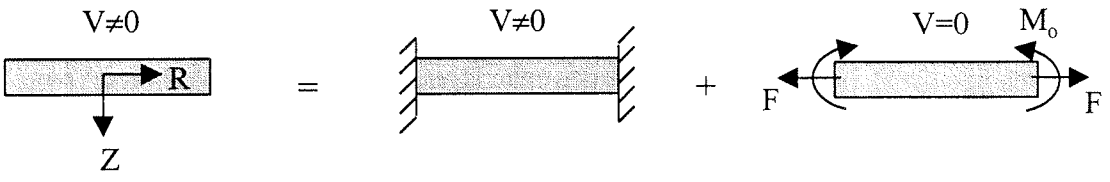

a) Unconstrained Gage b) Constrained Gage c) Mechanically Loaded Gage

Figure 13. Load equivalence (*2*).

4.1.2 Duomorph Response in Air

As a first step in the analysis, the response of the duomorph gage in air was modeled. The various considerations in performing this analysis are explained below. In the second step, the response of the gage after it was embedded into the asphalt medium was analyzed. Obviously, decisions taken regarding the element type, mesh refinement, and loading in the first step carry over to the second step.

Model Geometry
The ADART#1c is a circular gage 25 mm in diameter and 0.51 mm thick (two 0.19 mm thick piezoceramic layers and a 0.13 mm thick steel shim). Since the duomorph is essentially a thin solid of revolution, axisymmetric analysis was assumed to be appropriate. The symmetry afforded by the model was taken advantage of and only one-half of the model was considered for meshing.

Element Selection and Meshing
Since the duomorph is only operated in flexure mode, finite element types that can accurately represent this mode of deformation were chosen from the ABAQUS element library along with other elements to provide a basis for comparison. Three different axisymmetric element types were utilized to solve the problem including 4-noded bilinear elements (CAX4), 4-noded bilinear, incompatible mode elements (CAX4I), and 8-noded biquadratic elements (CAX8). Incompatible mode elements are first-order elements that are enhanced by incompatible modes to improve their bending behavior. The active degrees of freedom in all these element types are the radial and axial displacements, u_r and u_z, respectively.

Three different meshes were configured with each element type to form a matrix of 9 finite element meshes. The coarsest mesh comprised of 45 elements and the finest mesh had 1140 elements. Since the maximum strain gradients from the applied edge moments are anticipated to occur closer to the line of symmetry, care was taken in the mesh development to bias the nodes closer to this boundary in each of the 9 meshes.

Material Definition
The difficulty in obtaining piezoelectric material inputs has already been discussed in a preceding section. Since the problem has been converted to the mechanical domain, the only inputs required for the analysis are the Young's modulus and Poisson's ratio for the steel shim and the piezoceramic layers. For the purposes of this study, the piezoceramic and steel layers were modeled as isotropic, linear elastic materials. The material properties used in the analysis are given in table 5. Note that, for the piezoceramic layer, the manufacturer supplied Young's modulus values in the 31 direction, E_{31}, was used. E_{31} is most appropriate because it represents the material property when the applied electric field is along the polarization axis and the resulting deformation is perpendicular to it as is the case when the ADART#1C duomorph is in operation.

Table 5. ADART#1C gage material properties.

Material Type	Young's Modulus	Poisson's Ratio	Mass Density
PSI-5A-S2 Piezoceramic material	$E = 5.7x10^{10}$ Pa	0.30	7750 kg/m^3
Stainless steel	$E = 2.1x10^{11}$ Pa	0.25	7500 kg/m^3

Boundary Conditions

Assigning boundary conditions to the duomorph problem proved to be a difficult task. In reality, the duomorph is held in position in space by the electrical leads attached to it and the frame that houses it (see figure 6). However, it is not practical to translate this into a degree-of-freedom (d.o.f) based restraint required to perform the finite element analysis. In order to overcome this difficulty, the analysis of the duomorph's bending behavior by Briar et al. is once again consulted. In their idealization, Briar et al made a valid assumption that the neutral axis remains fixed in bending, as shown in figure 2, as the duomorph flexes back and forth under the applied AC voltage. This can be assured, in the finite element analysis, by preventing the nodes that lie on circumference of the duomorph, at the level of the neutral axis from translating in a direction perpendicular to the plane of the neutral axis.

The boundary conditions applied to the model define symmetry at the left edge (see figure 14[a]) (radial displacement, $u_r = 0$) and restrict rigid body motion at point B (axial displacement, $u_z = 0$).

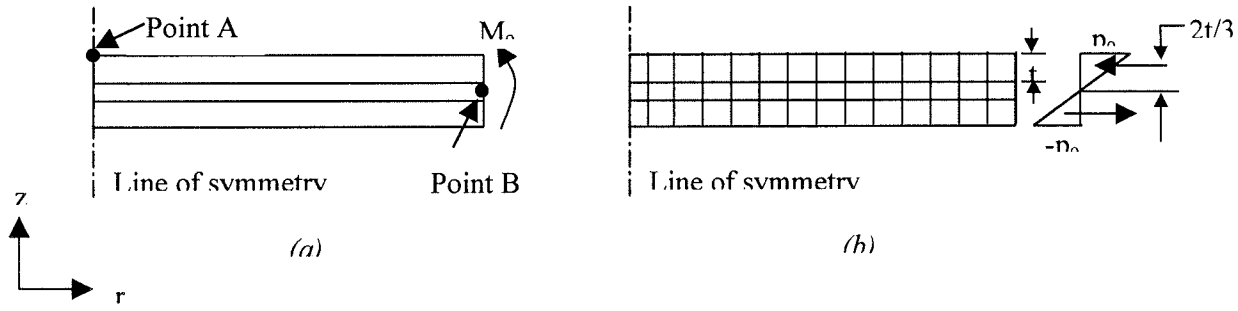

Figure 14. Applying an edge moment to the axisymmetric finite element mesh.

Loading

As discussed previously, edge moments are applied to the finite element mesh in place of the electrical loads. However, the degrees of freedom needed to apply rotations or moments at nodes are not active in axisymmetric analysis. Therefore, prior to the application of the load, the edge moment had to be converted to equivalent non-uniform element edge loads as shown in figure 14. The edge loads were varied sinusoidally at 1.59 Hz to simulate the laboratory application of the AC voltage of similar frequency.

Another challenge in the analysis was to determine the magnitude of the force p_0 that produces an edge moment corresponding to an AC voltage of 120 $V_{p\text{-}p}$ used to drive the duomorph in the laboratory. This was determined iteratively by continually matching lab measured bending strain at point A, in figure 14, with those from the finite element analysis produced by a succession of arbitrarily assumed moments. The magnitude of force p_0 that produced a strain closely matching the laboratory-measured value was assumed as the mechanical equivalent of the electrical load. This was held constant for all the finite element meshes. The nonlinearly distributed edge

traction shown in figure 14(b) is then converted to nodal traction vector by the finite element program for each of the finite element meshes under consideration.

Results and Discussion

A steady state dynamic analysis was performed using the ABAQUS *STEADY STATE DYNAMICS procedure. The frequency of loading was 1.59 Hz. The two parameters of interest to the finite element calculations, the peak bending strain at the center of the DART gage (ε_{11}) and the shift in the gage response with respect to the drive signal when the peak strain is achieved, were computed. As expected, the phase shift was zero degrees in all cases. The non-dimensionalized bending strains for the each of the 9 finite element meshes are shown in figure 15. The laboratory measured ADART#1c bending strain at the gage center was used to non-dimensionalize the calculated strains.

Since the load on the finite element meshes has already been pre-adjusted to produce the laboratory measured strains, matching the calculated strains with measured strains will be a trivial exercise. However, the results shown in figure 15 should be used to infer the suitability of the element types considered in performing the duomorph strains. It can be inferred from the figure that the finite element mesh with CAX8 elements was able converge to the exact solution even with as few as 45 elements, whereas, the mesh with CAX4 elements converges to the exact solution only at 1440 elements. The mesh with CAX4I elements also converges with a small

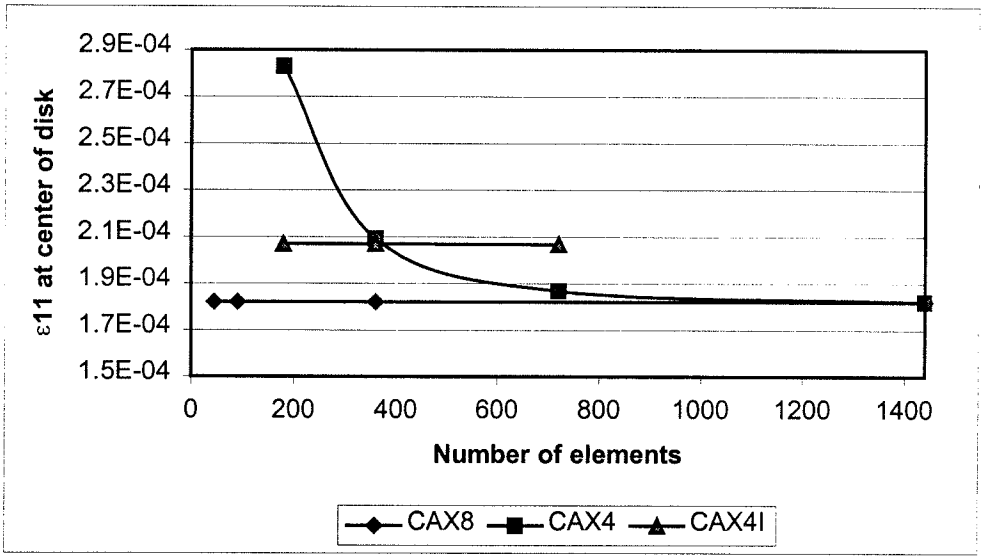

Figure 15. Mesh convergence study for the duomorph gage.

number of elements but shows a "softer" response compared to the mesh with the CAX8 elements.

Based on this analysis it can be concluded that the CAX8 elements are appropriate to accurately model the duomorph bending. Further proof of the ability of these elements can be obtained by comparing the non-dimensionalized deflection profile of the outer bottom edge of the duomorph with profiles determined using interference holographic analysis performed by Briar et al. for another duomorph with similar dimensions and loading. This comparison is shown in figure 16.

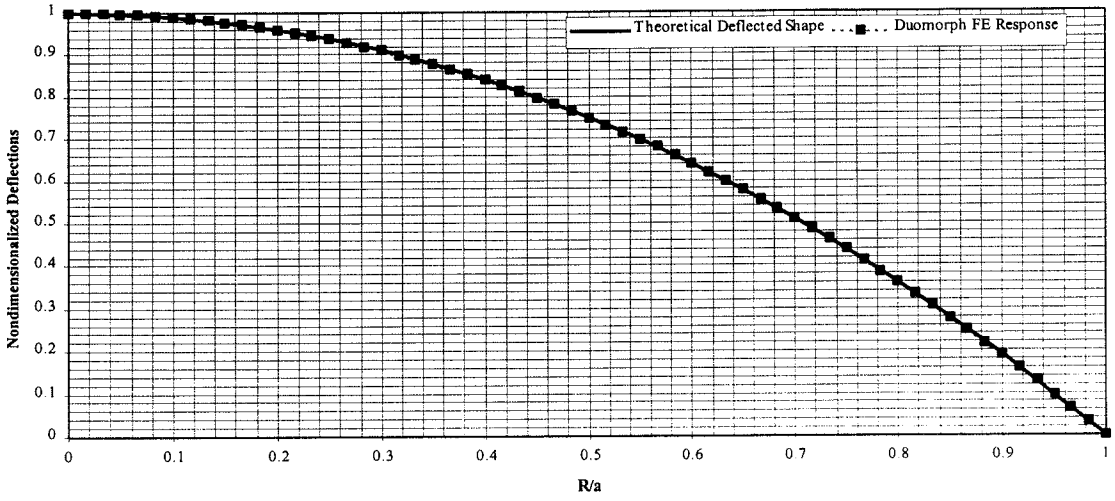

Figure 16. Nondimensional deflected shape comparison.

Another type of element that was considered for modeling the duomorph behavior was the laminated axisymmetric shell element SAX1, which is a 2-node thin or thick linear shell using three degrees of freedom per node. Shell elements were deemed appropriate considering the thinness of the plate and the fact that the plate when subject to the moments described is expected to simultaneously display bending as well as membrane stresses—a characteristic of shell behavior. Results from the usage of this elements were close to those from the CAX8 idealization of the ADART#1c gage. However, some potential complexities such as the use of contact elements and incompatible element types were perceived when the duomorph model in air is extended to incorporate embedding in the asphalt medium. Therefore, the CAX8 elements were pursued in the next stage of analysis.

4.1.3 Duomorph Response in Asphalt

In the second step, the response of the gage after it was embedded into the asphalt medium was analyzed. The various considerations in modeling this response are presented below. Obviously, decisions taken regarding the element type, mesh refinement, and loading for the duomorph in the first step were carried over to the second step.

Model Geometry

The cylindrical asphalt specimen with a circular gage embedded in it lends itself well to axisymmetric analysis. The dimensions of the tank and PAV specimen have already been discussed under section 3. Figure 17 shows the arrangement of the DART gage within a tank

asphalt specimen. The symmetry afforded by the model was once again taken advantage of and only one-half of the geometry was considered for meshing.

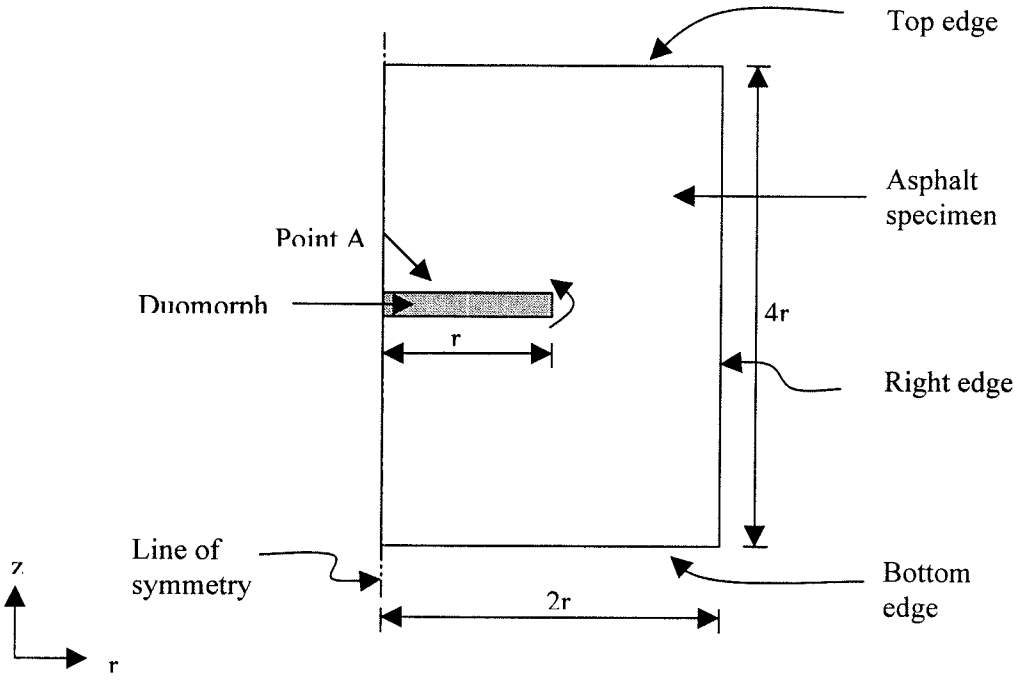

Figure 17. Geometry of asphalt specimen with embedded duomorph.

Element Selection and Meshing

Since CAX8 type elements were found to be adequate to model the gage behavior, they were chosen to model the asphalt medium as well to ensure element compatibility. The interface between the duomorph and the asphalt is meshed continuously, i.e., contact elements were not used. This is a valid approach since the duomorph gage and the asphalt cement surrounding it are not expected to debond over the range of temperatures and frequencies considered in this analysis. Recall that the gage is embedded in the asphalt when it is hot ensuring a good bond between the two materials. The advantage of using the CAX8 element type for the duomorph gage analysis over the shell elements is also obvious at this point. The use of the SAX1 type shell elements would have entailed a computationally intensive contact analysis due to the incompatibility in the element types.

The finite element mesh, loading, and boundary conditions of the duomorph gage from the prior analysis were retained. A nonuniform mesh was generated over the asphalt specimen using CAX8 elements taking care to bias the nodes in both directions to produce a finer mesh around the duomorph since this is the region of interest. Three different mesh sizes comprising of 2150, 3780, and 5580 elements respectively were generated to check for convergence.

Material Definition

The duomorph problem in asphalt can be modeled using the frequency-domain viscoelastic material model in ABAQUS since the excitation of the asphalt due to the duomorph falls under the realm of steady-state small vibration analysis. The frequency-domain viscoelastic material model in ABAQUS is isotropic and linear which is adequate to describe asphalt binder behavior.

Therefore, the asphalt binder was modeled as a linear viscoelastic material using the *VISCOELASTIC option in ABAQUS. The viscoelastic material inputs to the model can be input in a tabular form as pairs of modulus versus frequency. Both the real and imaginary part of the complex shear modulus, G' and G", must be entered in the normalized form. The normalization can be achieved as indicated in equations 4 and 5 below:

$$\omega R(g^*) = G''/G_\infty \qquad \text{Eq. 4}$$

$$\omega I(g^*) = 1\text{-}G'/G_\infty \qquad \text{Eq. 5}$$

G_∞ is an additional input to the material model and represents the long-term stiffness of the material. This must be defined in ABAQUS using the option *ELASTIC. In theory, this value corresponds to the shear modulus of the material when the loading frequency is infinity. ABAQUS reads the tabular frequency response input data and converts it into a power law equation for convenience of computation. Note that the definition of the components of the bulk modulus, required to complete the material characterization, is not required in this analysis since the material is near incompressible.

The modulus frequency pairs for the asphalt binders under consideration were determined by performing frequency and temperature sweep testing using the PAAR-Physica® research grade DSR. Data was obtained over a frequency range of 0.1 Hz to 100 Hz for each of the asphalts and over a temperature range of 5°C to 60°C. Figure 18 presents an example of the complex shear modulus response at various frequencies and test temperatures determined using the DSR for the AC-10 grade asphalt binder. Similar data were collected for the storage modulus, G', loss modulus, G", and the loss tangent, tanδ for each of the three asphalt under consideration.

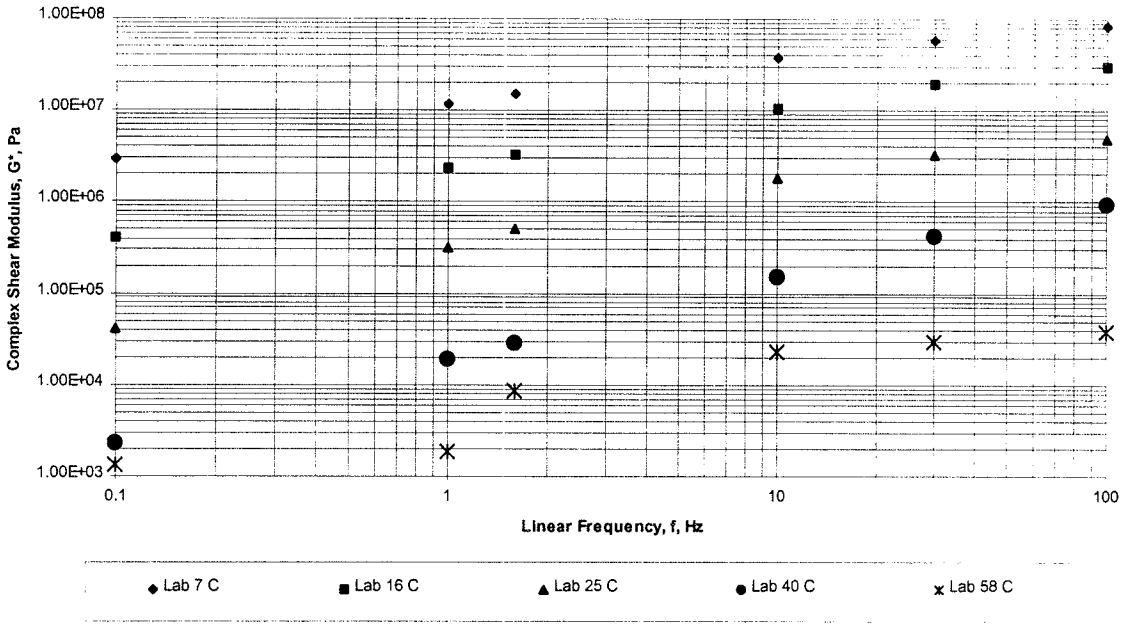

Figure 18. Example plot of DSR output—G* vs. frequency.

The long-term shear modulus for each of the curves in figure 18 was estimated by extrapolation to a frequency of 10000 Hz. The logic behind choosing this frequency was that it is approximately four decades away from the frequency of interest—1.59 Hz. Further, the G* vs.

frequency curves tend to flatten out and converge at this high frequency. The Poisson's ratio of the asphalt binder was assumed as 0.49. The material properties of the duomorph gage have been discussed in section 4.1.2.

Boundary Conditions
Since symmetry afforded by the model was utilized for computational efficiency, nodes lying on the axis of symmetry will obviously have symmetry conditions applied to them, i.e., $u_r = 0$. Recall that in the CAX8 type finite elements only translational d.o.f's are active. The cylindrical asphalt specimen with the embedded gage shown in figure 17 is placed in a glass container (see figure 6). Consequently, the restrictions imposed by the container on the asphalt specimen translate into displacement-based boundary conditions for the finite element model.

Since the nodes lying on the bottom edge of the specimen in figure 17 are prevented from translating in the z-direction, a displacement boundary condition of $u_z = 0$ is appropriate for these nodes. For nodes lying on the right edge of the specimen, since the radial displacements are restricted by the container, a boundary condition of $u_r = 0$ is applied for these nodes. Theoretically, these nodes are free to translate in the z-direction along the walls of the container. Finally, since the top surface of the specimen is unrestricted no displacement boundary conditions are needed on this face.

Loading
The only loading in the model is on the duomorph gage which has already been discussed in section 4.1.2. The magnitude of the edge moment determined for the duomorph analysis in air was held constant in the analysis. This provides a direct comparison of the duomorph response in air and in asphalt.

Mesh Convergence
The three meshes configured with varying degrees of mesh refinement were analyzed for mesh convergence using the boundary conditions and loading as defined here. The material definitions used in the analysis were those for the AC-10 tank binder tested at 16°C. The parameter under investigation for the mesh convergence study is the bending strain at the center of the duomorph (point A in figure 17). Based on this analysis, the following conclusions were arrived at:

- The bending strain solution converged quickly to a constant value. In fact there was no appreciable difference in the strain value between the three meshes.
- The contour plots of the strain field indicate that, in most instances, at a distance of about 2r to 3r on either side of the duomorph in the direction of motion (z-direction in figure 17), the strain magnitudes dissipated to negligible levels compared to the strain at point A.

Based on these finding a finite element mesh with 3780 elements was conservatively adopted for the analysis since some of the meshing characteristics of this mesh obeyed commonly followed rules of thumb for generating acceptable finite element meshes. For example, in this mesh care was taken to ensure that while transitioning from one element size to the next, the ratio of the adjacent element lengths was kept between 1.5 to 2.0 to ensure smooth displacement and strain gradients. Further, the largest element aspect anywhere in the mesh was in the vicinity of 5.0. Figure 19 presents the finite element mesh utilized for all further analyses.

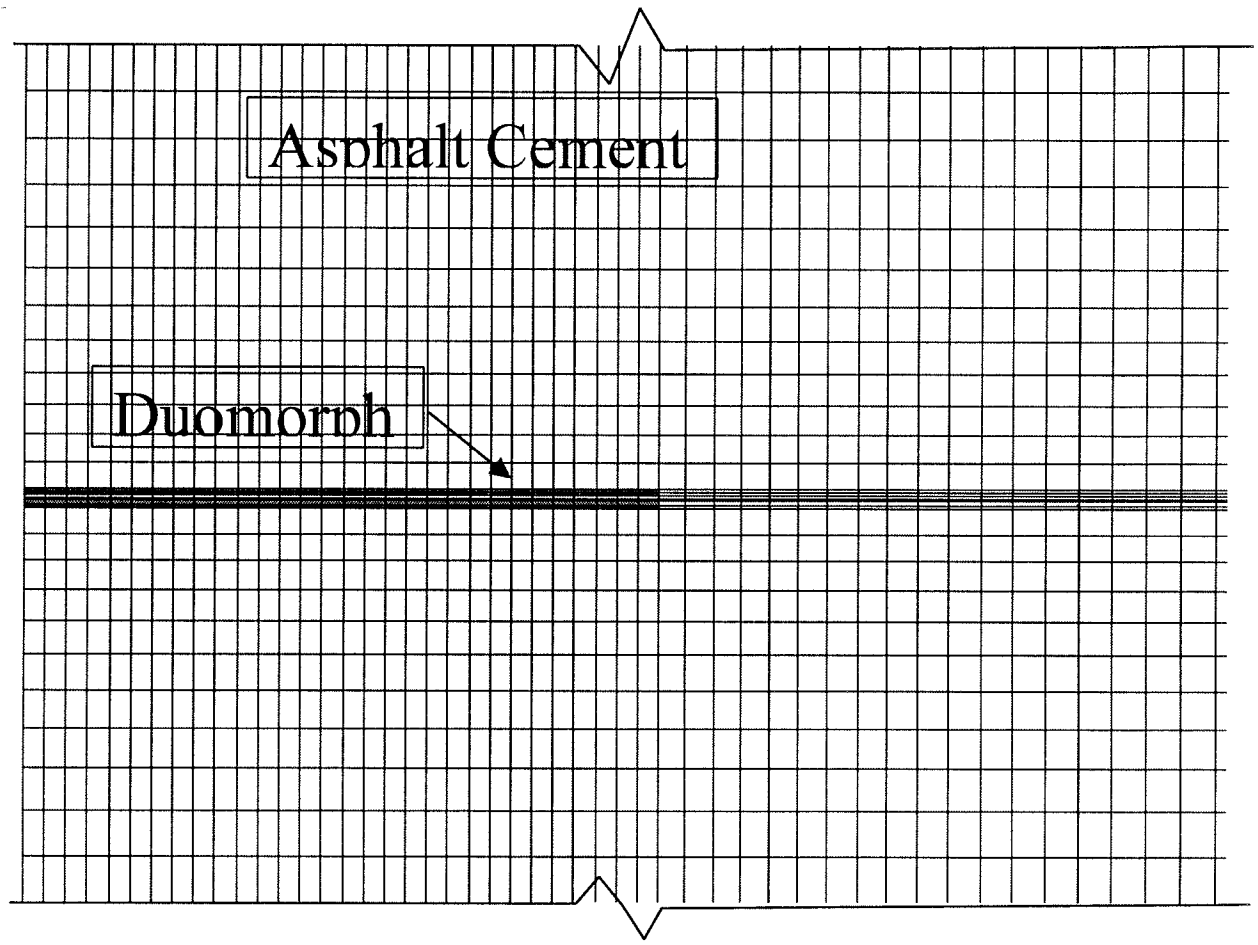

Figure 19. Finite element mesh utilized to model the duomorph response in asphalt.

Results and Discussion

Several finite element runs were performed for each of the three asphalt binders under consideration using the finite element mesh configured. Each run corresponded to a particular temperature for which the frequency-modulus curves were determined from the DSR for a given asphalt. The finite element output from each analysis was the maximum bending strain at the center of the duomorph gage and the corresponding signal shift. These maximum gage bending strain outputs in asphalt were divided by the previously calculated finite element values of maximum gage strain output in air to obtain a strain ratio. The strain ratio from each finite element run were then compared with those determined experimentally at the same temperature and under the same loading conditions for each of the asphalt binders. The comparisons between the finite element and laboratory strain ratios for AC-10, AC-20, and AC-40 binders are shown in figures 20 through 22.

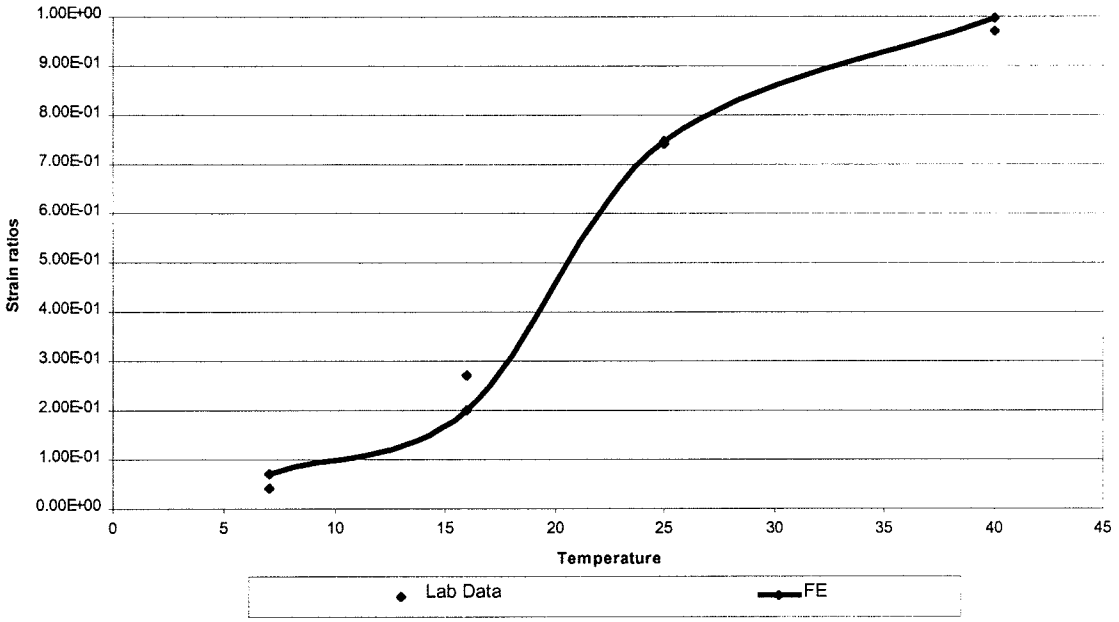

Figure 20. Comparison between finite element and experimentally determined strain ratios for AC-10 tank asphalt.

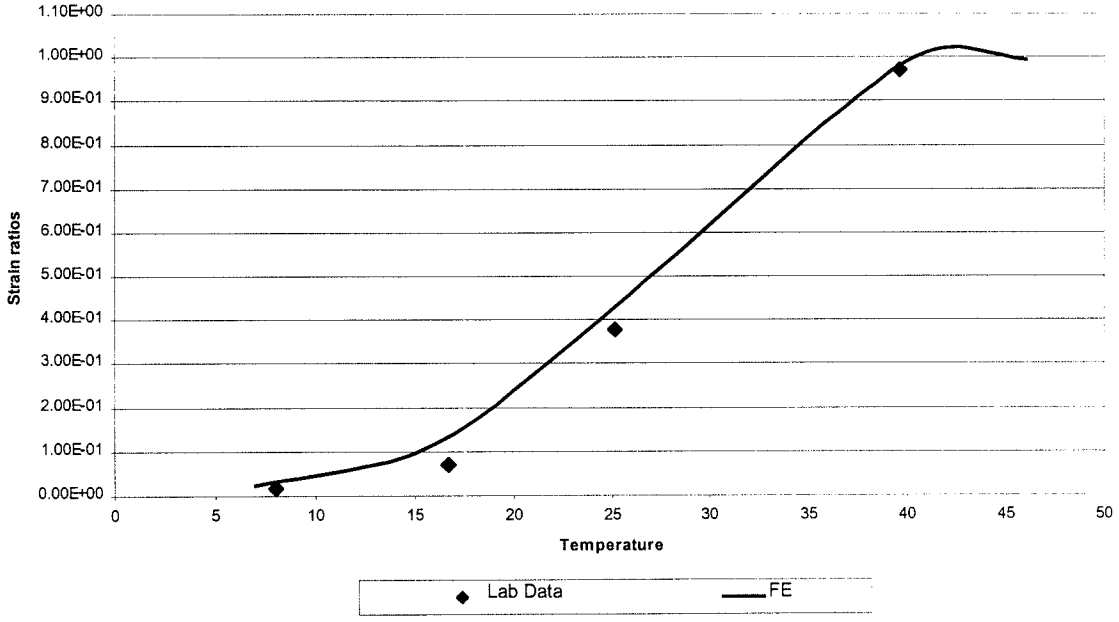

Figure 21. Comparison between finite element and experimentally determined strain ratios for AC-40 tank asphalt.

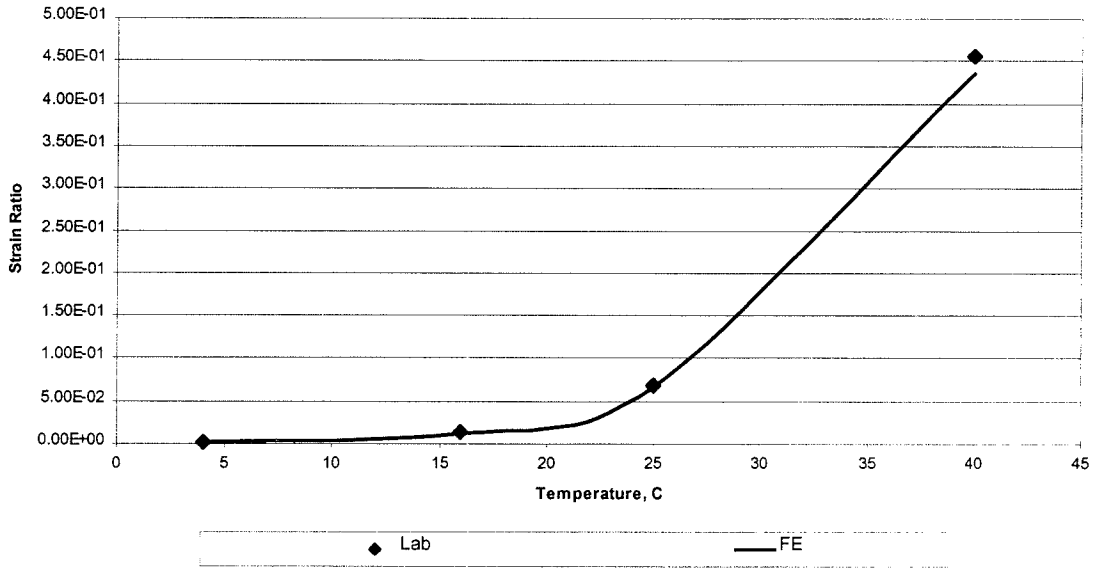

Figure 22. Comparison between finite element and experimentally determined strain ratios for AC-20 PAV aged asphalt.

Similar comparison plots for the signal shifts are presented in figures 23 through 25.

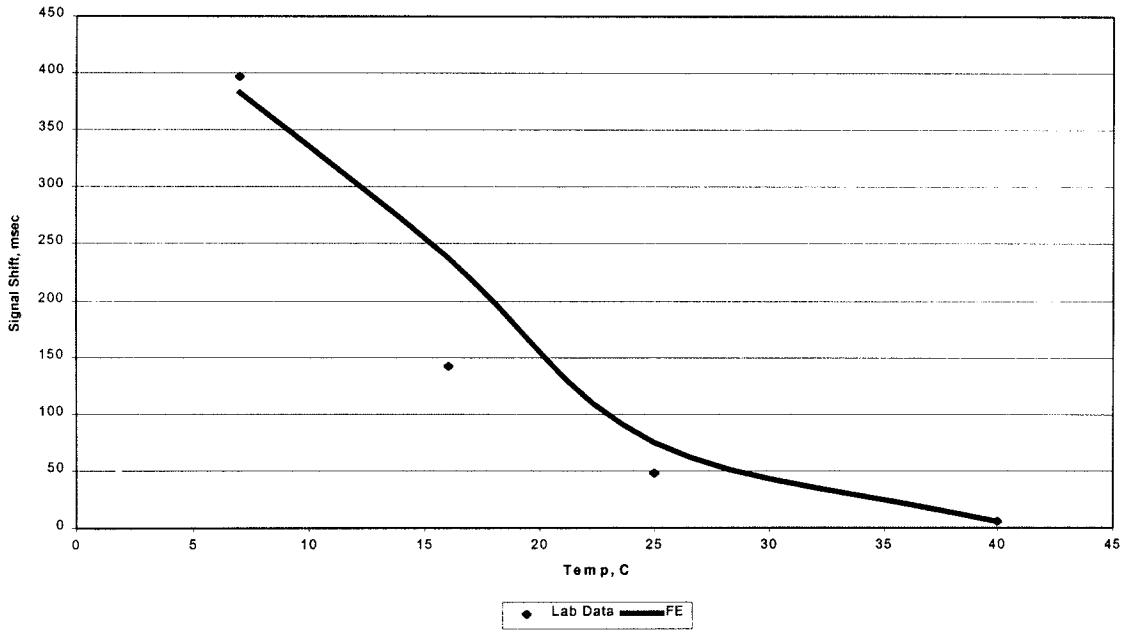

Figure 23. Comparison between finite element and experimentally determined signal shifts for AC-10 tank asphalt.

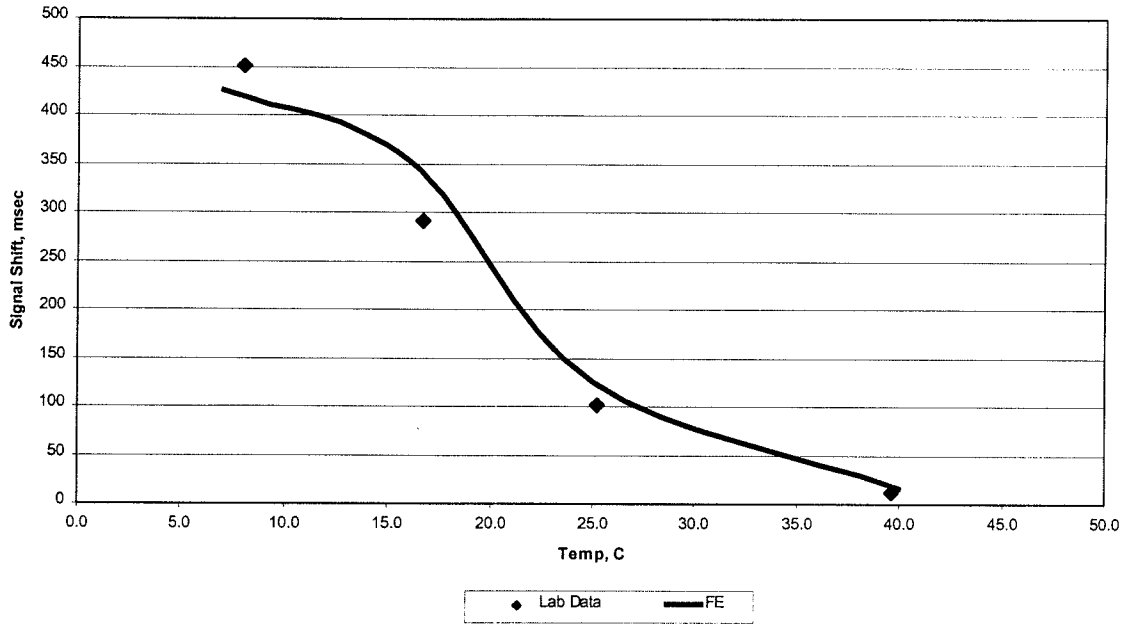

Figure 24. Comparison between finite element and experimentally determined signal shifts for AC-40 tank asphalt.

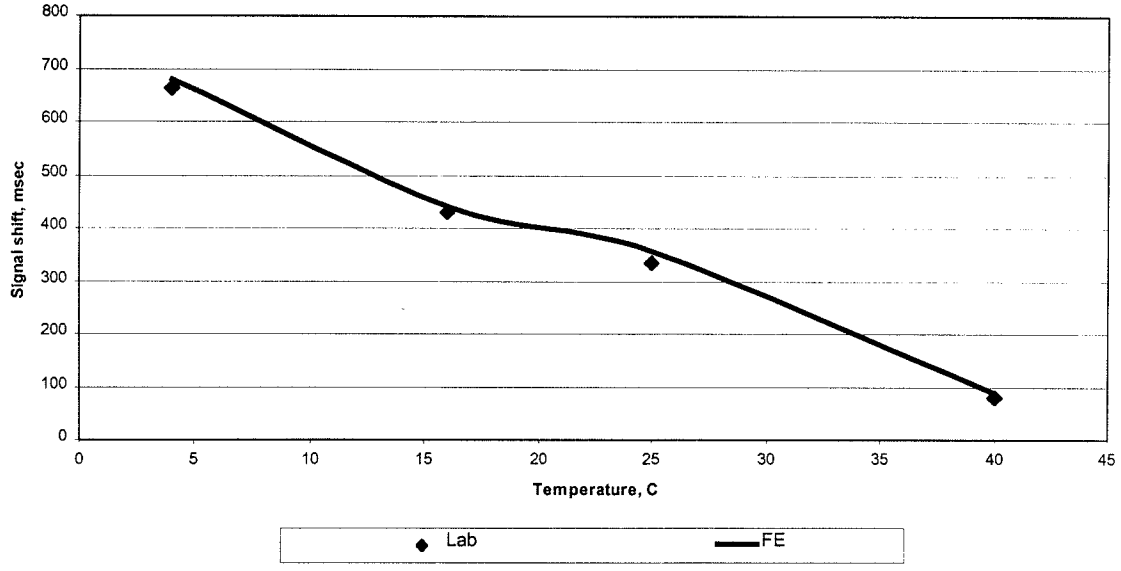

Figure 26. Comparison between finite element and experimentally determined signal shifts for AC-40 tank asphalt.

Two observations regarding the finite element model of the duomorph can be made based on the results presented:

- The observed trends in the outputs of the finite element model agree extremely well with the experimental data. This observation verifies the finite element model of the duomorph.
- The finite element outputs are validated by the experimental data. In all cases, the correlation coefficient between the observed and predicted value is in excess of 0.90 with a majority of the comparisons exceeding an R^2 of 0.95.
- The limitation of the ADART#1c gage to provide reasonable stiffness data in the laboratory beyond 40°C in AC-10 asphalt and 45°C in AC-40 tank asphalts is confirmed by the analysis. However, the range of temperature over which the ADART#1c gage can produce valid data increases with increased stiffness of the binder as evidenced by the data from stiffer AC-20 PAV aged asphalt.

As was noted in the discussion at the end of section 3.2, using a gage with a lower flexural rigidity can increase the sensitivity of the duomorph at the high temperatures which produce low stiffnesses in the binder. This fact is demonstrated in the analysis presented in figure 26 where the material properties of a soft asphalt were held constant and the gage flexural rigidity was varied until satisfactory strain ratios were obtained. The disk flexural rigidity required to obtain a strain ratio of 0.4 in a "soft" asphalt is within the realm of practical engineering piezoelectric materials. This aspect needs further investigation.

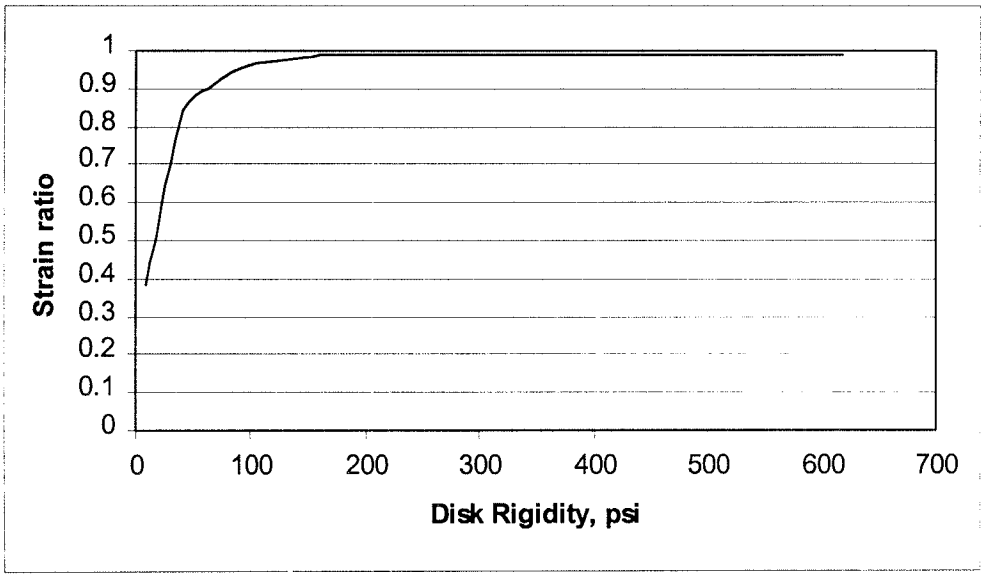

Figure 26. Analysis of the influence of duomorph gage flexural rigidity on the strain ratio.

6.0 SUMMARY, CONCLUSIONS, AND RECOMMENDATIONS

This NCHRP-IDEA project investigated the feasibility of using the Duomorph technology as an asphalt binder test device to determine the Superpave binder properties which are essentially a viscoelastic characterization of the binder. The first phase established the ability of the device to function properly with sufficient durability to warrant further investigation directed toward the development of a field ready device. The testing and evaluation clearly indicated the need to develop a more robust viscoelastic analysis procedure to replace the elastic solution first proposed by Briers, et. al., to extend the computational range to include the property ranges typically exhibited by asphalt cement binders in the normal temperature range encountered in specification testing.

In the second phase of the study, toward the development of a final testing assembly, the sensor electronics and operation of the duomorph gage were formalized. Testing was performed over a broader range of asphalt stiffnesses and the data outputs were analyzed for consistency. It was shown that the duomorph is sensitive to changes in both asphalt binder stiffnesses and phase angles. The data collected from the duomorph is highly repeatable. However, there are certain practical limitations to the stiffness range over which the duomorph produces reliable data.

A viscoelastic finite element model was configured to simulate the duomorph responses determined in the laboratory. Axisymmetric 8-noded elements were used in the model. The problem domain was shifted from a piezoelectric domain to a mechanical domain. The Dynamic Shear Rheometer was used to test three asphalt binders to determine complex moduli over a range of temperatures and frequencies. Using these data for comparison, the duomorph outputs from the finite element analysis compared extremely well with the laboratory data, validating the modeling approach. The limitation to the duomorph operation noted in the experimental analysis was confirmed by the theoretical investigation. Preliminary analysis indicating what can be done theoretically to extend the valid range of the duomorph operation proved promising and will need to be investigated further.

The development and verification of this finite element model, and the finalization of equipment consumed the phase II work effort. The work clearly establishes the ability of a viscoelastic based analysis scheme to more accurately predict the viscoelastic properties of an asphalt cement binder.

The following recommendations are currently under development to accomplish the stated objectives of producing a field ready device with internal data collection and reduction capability:

- Utilize the finite element model, validated in this phase to develop a new data reduction scheme for the DART device. This will entail conducting a parametric study using the finite element model to compute a database of gage responses from assumed asphalt material properties and performing an "inversion" using either a regression model or neural networks.
- Validate the new data reduction scheme and calibrate the model if necessary.
- Investigate new piezoelectric materials to expand the capabilities of the duomorph.

REFERENCES

1. Briar, H.P., Bills, K.W. "Development of an In-Situ Transmitter for Solid Rocket Propellant Surveillance". Report No. AFRPL-TR-72-93, December, 1972.
2. Briar, H.P., Bills., K.W., Schapery, R.A. "Design and Test of the Operational In-Situ Gage for Solid Rocket Propellant Surveillance". Report No. AFRPL-TR-76-36, June, 1976.
3. Grosz, F.B. DUONOMO and DUO_CALC: Computer Programs for Duomorph Data Reduction, Copyright (c) by Francis B. Grosz, *Personal Communication*, 1995.
4. Carpenter, S.H., J. Mallela. "Development of a Self-Contained Portable Device for SHRP Binder Testing: Field QC/QA Testing with the Duomorph". Final Report, Prepared for NCHRP under Contract NCHRP-94-ID017, Transportation Research Board, Washington D.C., 1996.